Monte Carlo Study of the Aqueous Hydration of Dimethylphosphate Conformations

B. Jayaram,* M. Mezei, and D. L. Beveridge†

Department of Chemistry, Hunter College of CUNY, New York, New York 10021

Received 14 October 1986; accepted 10 December 1986

Monte Carlo computer simulations were performed on dilute aqueous solutions of the dimethylphosphate anion and the sodium dimethylphosphate ion pair, with the two phosphodiester torsional angles in the gauche–gauche, gauche–trans, and trans–trans conformations. The structural and energetic aspects of the aqueous hydration of each molecule were analyzed in terms of quasi component distribution functions based on the proximity criterion and partitioned into ionic, hydrophilic, and hydrophobic contributions to facilitate an understanding of the hydration pattern and conformational trends in these multifunctional solutes. Special attention was also paid to methodological issues affecting hydration, such as statistical uncertainty in the determined hydration indices, choice of partial atomic charges for the solute atoms, and solute–water interaction potentials adopted in the simulations. The results showed that gauche–trans and gauche–gauche forms are equally favorable for the dimethylphosphate anion with the trans extended form destabilized by hydration. The sodium dimethylphosphate ion pair hydration energetically favors the trans–trans conformation.

I. INTRODUCTION

The structures of nucleic acids show considerable conformational flexibility and are known to be sensitive to hydration and ionic strength. The phosphate moiety, $-O-PO_2^--C-$, bears the anionic charge in each nucleotide unit and environmental effects are expected to be very strong in this region. The phosphodiester torsion angles are thus an important conformational coordinate in nucleic acid structure. We report herein a theoretical study of the aqueous hydration of the phosphodiester group, the effect of hydration, and the influence of counterion on the conformational preferences of the phosphodiester torsion angles. This study is based on (T, V, N) ensemble Monte Carlo mean energy computer simulations on the dilute aqueous solution of the dimethylphosphate anion, $[DMP^-]_{aq}$, and the sodium dimethylphosphate ion pair, $[Na^+DMP^-]_{aq}$, at a temperature of 25°C and experimental density.

II. BACKGROUND

Dimethylphosphate at physiological pH is found predominantly in the anionic form. The conformations of DMP^- can be specified in terms of the torsional angles α (O—P—O—C) and ζ (C—O—P—O),[1] following IUPAC notation. The angles α and ζ are identical to w and w' assigned to the phosphodiester torsions in some of the earlier literature. Both α and ζ follow roughly a threefold potential with minima in the regions of gauche$^+$ (g^+), trans (t), or gauche$^-$ (g^-). In this account, we contract the notation for the specification of conformation for DMP^- to simply "$\alpha\zeta$", i.e., gg, gt, or tt. These conformations are depicted in Figure 1. In the solid, DMP^- with ammonium counterion crystallizes with $\alpha = \pm 57.5°$ and $\zeta = \pm 62.4°$, a gg conformation.[2] Crystal structure data on phosphodiester torsion angles for various dinucleotides reveal a strong preference in these systems for gauche values of α and ζ, presumably stabilized by anomeric effects. A recent search of the Cambridge crystallographic data bank[3] turned up 45 structures with gg conformations versus only six structures exhibiting a combination of gauche and trans, i.e., gt, or tg values. The

*Present address: Department of Biochemistry and Molecular Biophysics, Columbia University, 630 West 168th Street, New York, NY 10032.

†Present address: Department of Chemistry, Wesleyan University, Middletown, CT 06457.

Journal of Computational Chemistry, Vol. 8, No. 7, 917–942 (1987)

CCC 0192-8651/87/070917-26$04.00

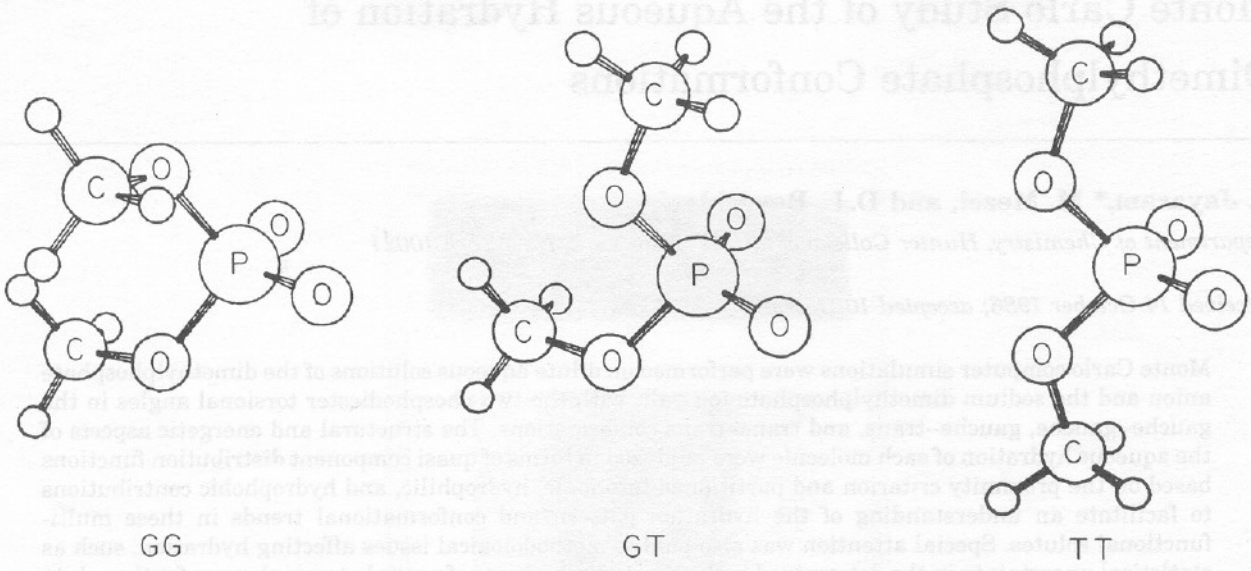

Figure 1. The structure of dimethylphosphate anion in *gg*, *gt* and *tt* conformations.

tt form seems to occur extremely rarely in phosphodiester torsion angles.

Information on the conformational preferences of DMP^- in solution comes from IR, Raman, and NMR spectroscopic studies. Shimanouchi, Tsuboi, and Kyogoku[4] interpreted the IR spectrum of $Ba^{2+}(DMP^-)_2$ and the Raman spectrum of Na^+DMP^- in aqueous solution by means of normal coordinate calculations and concluded that the *gg* form was the likely conformation for DMP^- in both solid and solution. However, conformational analysis of DMP^- based on depolarized Rayleigh scattering by Garrigou-Lagrange et al.[5] suggested that extended rotational isomeric states of DMP^- in water were highly populated.

Proton NMR is insensitive to changes in the α, ζ torsions, but ^{31}P NMR proves to be a useful probe. Gorenstein et al.[6] investigated the ^{31}P chemical shifts of DMP^- and related compounds in aqueous solution as a function of temperature, in conjunction with studies of nucleic acid conformation. The ^{31}P resonance shifts downfield as a function of temperature. This was interpreted by an increase in the Boltzmann population of *gt* and possibly *tt* conformers with increasing temperature. By inference, the preponderance of *gg* conformation of DMP^- at lower temperatures, including ambient, was indicated. On the other hand, Lerner et al.,[7] in their recent report on solvation effects on ^{31}P NMR chemical shifts and IR spectra of phosphate diesters in water and mixed organic solvent systems, interpreted changes in ^{31}P chemical shifts with increasing concentration of nonaqueous solvents as due to changes in the phosphate hydration rather than conformational changes. They further adduced the "blue shift" of the antisymmetric stretching frequency of the anionic O—P—O group as corroborative evidence.

Extensive research has been reported on the calculation of conformational preferences in phosphodiester torsional angles in DMP^- and related compounds in the free space approximation. Some early studies[8,9] with empirical potential functions favored the extended structures involving *t* forms of α and ζ, while others[10] favored gauche forms. Investigations based on extended Huckel theory[11] and PCILO method[12] on model compounds favored trans and gauche forms, respectively. Quantum mechanical calculations by Newton[13] on the α, ζ conformational energy map showed $gg < gt < tt$, with *tt* destabilized by some 7 kcal/mol. Recently developed potential energy functions[14–17] effectively incorporate the interactions between the lone pairs on the ester oxygens, destabilizing the extended forms relative to gauche form.

Perahia, Pullman, and Saran[18] showed the (α, ζ) energy surface to be sensitive to assumptions about molecular geometry. Subsequently, Perahia and Pullman[19] and Gorenstein et al.[20–22] demonstrated a significant correlation between the phosphodiester torsional angles and the ester oxygen O—

P—O bond angle, and found that a 4–5° reduction in O—P—O angle accompanied each phosphodiester torsional rotation from *g* to *t*. The conformational energy surface flattens when this is taken into account in calculations. All (α, ζ) conformations are then predicted to be thermally accessible to some extent, with a relative ordering in conformational energies of *gg* (0) < *gt* (+0.8–0.9 kcal/mol) < *tt* (+1.7–1.9 kcal/mol). This accentuates the possible role of hydration in deciding the relative conformational preferences for the phosphodiester torsion angles in solution.

Theoretical studies of the hydration of DMP^- by means of an exploration of the solute–water interaction energy hypersurface have been described in papers from several laboratories. Berthod and Pullman,[23] and Perahia, Pullman and Berthod,[24] using quantum mechanical calculations found extended and bridged structures for the DMP^- water monohydrate with stabilization energies of −20 to −28 kcal/mol depending upon whether or not *d*-functions were included in the atomic orbital basis set. PCILO calculations of Frischleder et al.[25] indicated that the strongest hydration occurs in the O—P—O plane bridging the anionic oxygens with an interaction energy of −27 kcal/mol for the $DMP^-(H_2O)$ complex. Gay and Vanderkooi,[26] performing CNDO/2 calculations, concluded that the lowest energy configuration (−20 kcal/mol) for $DMP^-(H_2O)$ was one with a linear hydrogen bond in which the atoms of H_2O were coplanar with the anionic oxygens of phosphate group. Alagona, Ghio, and Kollman[27] in their quantum mechanical and molecular mechanical studies on the DMP^- monohydrate found the bridged structure for water to be more stable than the linear structure by about 5–6 kcal/mol. More extensive "solvation site" studies were reported by Pullman, Berthod, and Gresh,[28] who enumerated possible DMP^- monohydrate structures. From these calculations they predicted that six waters would be found in two "circular zones of attraction" near the anionic oxygens and perpendicular to the P—O bond.

Corongiu and Clementi[29] and subsequently Clementi, Corongiu, and Lelj[30] studied the interaction of a single molecule with diethylphosphate anion and with the nucleic acid backbone model $MeCH_2—C—O—PO_2—O—CH_2Me$ using quantum mechanical calculations. Contour plots revealed an energy minimum of −24 kcal/mol for DEP^- and −18 to −20 kcal/mol for the backbone fragment, in "Region A" which corresponds to the anionic oxygen zone of attraction of Pullman et al. Another region called "B," in the ester O—P—O region, was also noted with binding energies apparently of a similar magnitude. The results of the calculations were used to construct an analytical potential energy function for these systems.

Clementi et al. used this analytical potential function in conjunction with a corresponding water–water potential to determine minimum energy structures for clusters of first four and then ten waters with DEP^- and with their nucleic acid backbone prototype and the results were mainly pertinent to phosphate hydration. They found their Region A to be preferentially populated and involved a single well-directed hydrogen bond pointing towards the two anionic oxygens, and that minimum energies were obtained by optimizing water–solute interaction at the expense of water–water interactions. However, the detailed structure of the small cluster was found to depend strongly on the number of waters considered, 4 to 10 in these studies.

The question of polyhydration of DMP^- was taken up in a more elaborate study by Pullman, Berthod and Gresh.[31] The essential trihydrate structure around each anionic oxygen was maintained, however. An extensive study of polyhydration based on energy minimization was recently reported by Langlet, Claverie, Pullman, and Piazzola.[32] The $DMP^-(H_2O)_6$ hexahydrate complex was subjected to translational and rotational energy optimization from various starting configurations. The solvation site model with three waters per anionic oxygen in the circular zone of attraction was recovered with only slight modification, the principal refinement being that 6–7 waters were admitted to the first shell as defined on a binding energy criterion. The energies of the various conformers were found to remain close even with the inclusion of waters. Studies on the systems $DMP^-(H_2O)_{30}$ and $DMP^-(H_2O)_{60}$ permitted a detailed analysis of the hydration complex, and also the "radially oriented" structure in the vicinity of the anionic O—P—O group and the "concentric structures," defined to

describe the hydration of DMP^- methyl groups. The terms "radially oriented" and "concentric" structures seem to be equivalent to the terms "ionic hydration" and "hydrophobic hydration" widely used to discuss the structural chemistry of aqueous hydration. Langlet et al. found that solvent effects on conformational stability in DMP^- were likewise small in the higher order water clusters.

A treatment of the aqueous hydration of DMP^-, HDMP, and H^+DMP^- has recently been carried out by Bleha, Mlynek, and Tvaroska[33] using an Onsager continuum model for the solvent. For DMP^-, the *gg* conformer was found to be preferentially stabilized in water as well as in free space, due primarily to the electrostatic dipolar contribution to the hydration energy.

The solvation shell model for the calculation of free energies of hydration, proposed by Scheraga and co-workers[34–36] and elucidated by Hopfinger,[37,38] assumes a model for hydration complexes of biological functional groups and subunits, which can be applied to DMP^-. The hydration numbers of solvation shell theory for DMP^- groups are: four for anionic O—P—O— group; two for each ester oxygen; and eight for each methyl group; leading to a value of 24 waters for the entire molecule in the extended *tt* form.

Monte Carlo simulation studies of the hydration of DMP^- have recently been reported in a preliminary form by Beveridge et al.,[39] and more extensively in a recent article by Alagona, Ghio, and Kollman.[40] Kollman and co-workers investigated the hydration of *gg* and *gt* conformations of DMP^- in the (T,P,N) ensemble. Partial atomic charges on the solute and the O—P—O valence bond angle were apparently treated as independent of conformation. Methyl groups were approximated by united atoms. The TIPS4P model was used to describe water–water interactions, and a 12-6-1 potential function for the solute–water interactions. About 23 water molecules were assigned to the first shell of DMP^- on a geometric criterion and were classified as belonging to strongly polar, polar, and apolar domains corresponding to ionic, hydrophilic, and hydrophobic regions. The average coordination number of three waters per anionic oxygen, and the absence of bridged water structures in the ionic region emerging from their simulation studies were in accord with quantum mechanical predictions of Pullman and co-workers described above. Computed enthalpies of hydration favor *gg* conformer over *gt* by 28 kcal/mol and this was ascribed to more attractive water–water interactions in the case of *gg*. Solute–water interactions and in particular ionic hydration favored the *gt* conformer in their study. Detailed comparison of the results of Alagona et al. with those of the present study creates for the first time a perspective on the sensitivity of simulation results to choice of potential function, assumptions concerning solute geometry, thermodynamic ensemble and method of analysis, and statistical uncertainty in the calculated results.

The influence of counterion on the hydration and stability of model compounds for nucleotides was reported by Rich and co-workers[41,42] in their ApU and GpC crystal studies. In ApU, one sodium ion was found to be bound to phosphate group, while the other was located in the minor groove region, bound to uracil and screened from the phosphate group by its first shell waters. In GpC, the sodium counterion was bound to the ionized phosphate group, exhibiting an octahedral coordination and was considered to be a major organizing structural element. Phosphodiester torsions were in *gg* conformation in both ApU and GpC.

Diethylphosphate anion crystallizes in *gg* conformation with barium counterion,[43] while with silver cation[44] it is in *gt* form. DMP^- with ammonium counterion as pointed out earlier,[2] crystallizes in *gg* conformation. Glonek and Wazer,[45] through their P-31 spin lattice relaxation studies on the aqueous solutions of several phosphate esters including DMP^-, concluded that the anionic phosphate group in presence of sodium and potassium cations was associated with closely lying waters, but structural details were not accessible.

Several theoretical studies involving quantum calculations on metal-phosphate complexes have addressed the problem of geometry and stability of the complexes and few the conformational problem. Nanda and Govil[46] performed CNDO/2 calculations on metal-cation interactions with DMP^-. Both sodium and magnesium counterions favored two-centered (bridged) interactions, with counterion in the plane of anionic PO_2^-

group, equidistant from the anionic oxygens. Conformational trends were reversed ($tt > gt > gg$) in the presence of counterion in their study. Pullman, Gresh, and Berthod[47] re-examined these trends with STO-3G *ab initio* calculations and found that the conformational trends were unperturbed ($gg > gt > tt$) by the presence of counterion. The bridge position for the counterion remained the stable form. Marynick and Schaefer[48] conducted *ab initio* calculations on a series of phosphate-counterion complexes including DMP^- (in *tt* geometry) with and without a water molecule attached to the metal ion. They inferred the contact interaction, with metal ion in C_{2v} symmetry with respect to the anionic oxygens of the phosphate group, as the most stable configuration for the metal-phosphate interactions. Pullman and Berthod[49] further investigated the effect of counterions on the molecular electrostatic potential of DMP^-. In their study, the counterion was placed on the bisector of PO_2^- at a distance of 2 Å from the anionic oxygens. The modified molecular potential indicated a strong decrease in the attractive nature of the PO_4^- group. Pack and co-workers[50] studied the geometric and charge transfer aspects of $M^+PO_4^-$ complexes. The preferred position for the sodium counterion was a bridged structure in the PO_2^- plane, in agreement with the earlier theoretical calculations.

Berthod and Pullman[51] subsequently considered the competetivity in binding of Na^+ and water to the DMP^- anion, through their studies on $Na^+DMP^-(H_2O)_6$ system. They proposed two modes of binding. One involved a direct binding of Na^+ to DMP^- and the other, sodium cation binding to phosphate anion through an intermediate water molecule, shared by both anion and cation. *Ab initio* calculations of Pullman et al.[52] involving these two modes of binding showed that the interaction energies were comparable, suggesting that both forms might contribute to the structure in solution.

Mlynek and Tvaroska[33] in their continuum study, referred to above, on H^+DMP^- intimate ion pair found *tt* to be the most stable conformation for the phosphodiester torsion angles.

Corongiu and Clementi[53] reported their cluster calculations on B—DNA fragment (12 base pairs, 24 sugar units and 22 phosphate groups) with one Na^+ placed fixed near the free oxygens of each PO_4^- group. They found an additional 1.5 water molecules per Na^+ in the first shell (R_c = 3 Å) of Na^+—B—DNA relative to B—DNA resulting in a highly dense and structured first shell termed an "ion induced compression effect," i.e., electrostriction in the conventional physical chemistry literature. Sodium cation on the average maintained an octahedral coordination in their study.

Overall, it is clear from the literature on DMP^- that solvent interactions are potentially a significant influence on conformational stability, and the hydration of the phosphate group is an important area for study in nucleic acids research. The theoretical study of DMP^- in water via simulation procedures is the appropriate place to begin, but a number of difficulties are anticipated. The quality of the potential functions is a matter of continuous concern in obtaining a satisfactory account of basic thermodynamic indices, the principal point of comparison with experimental studies as well as other results not as amenable to experimental verification. Intrinsic limitations in the precision of calculated quantities due to statistical uncertainties in ensemble averages formed over finite segments of a potentially infinite numerical realization exist, and are manifest especially in estimates of conformational energy differences where the "small differences in large numbers" problem is encountered. In charged systems or systems with charge separation, the periodic boundary conditions customarily assumed for simulations on aqueous system may be problematic. However, these issues cannot be addressed without carrying out a series of well defined simulation studies, effective computer experiments on the system, and gaining experience with the numerical problems and analyzing the results fully and critically. Thus, the purpose of the calculations undertaken herein is twofold: to describe the system, as well as possible and simultaneously to gain perspective on the methodology.

III. CALCULATIONS

Statistical thermodynamic (T, V, N) ensemble Monte Carlo simulations were carried out individually on dilute aqueous solutions of DMP^- anion and Na^+DMP^- ion pair in the *gg*, *gt*, and *tt* conformations, using a modified Metropolis procedure[54] incorporating force

bias method[55] and preferential sampling[56] for convergence acceleration. The system for study, in each case, consisted of 216 rigid particles, one DMP (anion/ion pair), and 215 water molecules. The computer experiment was performed at 25°C, and a density determined from the experimentally observed partial molar volume for water and derived partial molar volume of 59.3 mL/mol for DMP^-,[57] and 53.1 mL/mol for the ion pair.[57,58] The condensed phase environment of the system was simulated by face centered cubic boundary conditions which provides here in excess of two hydration shells for the solute. Convergence characteristics and statistical error bounds on each of the calculated quantities were monitored by the method of batch means.[59] Full details of the Monte Carlo procedure as applied in this laboratory are described in a recent article by Mehrotra et al.[60]

The N-particle configurational energies of the system were calculated under the assumption of pairwise additivity in intermolecular interactions using potential functions determined from *ab initio* quantum mechanical calculations. Water–water interactions were modelled by MCY potential[61] developed by Matsuoka et al., and solute–water interaction by an analytical potential function developed by Clementi and co-workers. The performance of MCY water–water potential has been extensively documented in the recent literature,[62] and is known to give good agreement with experimental radial distribution functions in simulations carried out at experimental density. The shortcomings arise in the neglect of cooperative effects, estimated to incur a 13% error in computed internal energies for $[H_2O]_1$ and an inordinately high calculated pressure indicative of deficiencies in the curvature of the potential. The latter problem is kept under control by working consistently with experimental densities in (T, V, N) ensemble simulations.

The DMP^--water interactions were computed using the 12-6-1 analytical potentials developed from quantum mechanical calculation by Clementi et al.[30] The geometry for DMP^- adopted in our study, was that of Gorenstein and co-workers.[22] The (α, ζ) torsional angles were *gg* (60°, 60°), *gt* (60°, 180°), and *tt* (180°, 180°). The OPO valence angles for the *gg*, *gt*, and *tt* conformations were taken to be 103.4°, 97.5°, and 92° respectively, following Gorenstein et al.[22] Net atomic charges for each of the conformers of DMP^- were computed using the Gaussian-80 system of programs[63] and the atomic orbital basis sets given by Matsuoka et al.,[64] and consistent with the potential functions. We have looked at the behavior of this basis set for the conformational preferences of DMP^- in vacuum for both fixed[13] and optimized geometries.[22] By fixed geometry a constant value of 102.6° is meant for the O—P—O valence angle in all three conformations and by optimized geometry, an optimized OPO valence angle for each conformation the values of which are quoted above. The energies relative to *tt* are −1.81 and −3.36 kcal/mol for *gt* and *gg*, respectively, in the fixed geometry, and 0.26 and 1.58 kcal/mol for the optimized geometry; the increased stability of the extended forms in vacuum upon optimization of the O—P—O valence angle is seen to be reproduced. A slice of the potential energy hypersurface for the $DMP^-(g,g) \cdot H_2O$ interaction calculated from the 12-6-1 potential function in the PO_1O_2 plane is given in Figure 2. The energy minimum is in the plane of anionic oxygens and the interaction is worth ca. −21.6 kcal/mol. This surface also indicates that an in-plane bridge structure is more stable than a coplanar sequential H-bond by about 2 kcal/mol. Next in interaction strength are the planes of PO_1O_3 and PO_2O_4 with E ca. −16 kcal/mol, followed by the PO_3O_4 plane with E ca. −11 kcal/mol.

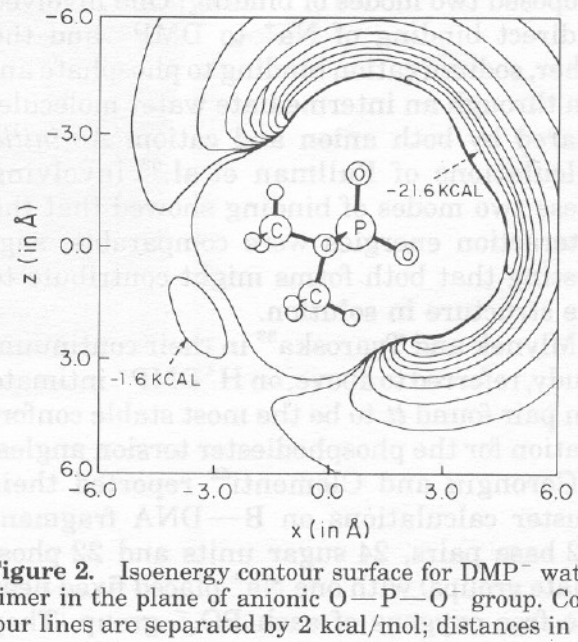

Figure 2. Isoenergy contour surface for DMP^- water dimer in the plane of anionic O—P—O^- group. Contour lines are separated by 2 kcal/mol; distances in Å.

Bridged structures are predicted to be the most stable structures for the *gt* and *tt* conformations as well. The stability of the bridged structures for the monohydrate complexes of DMP^-, as well as the interaction energies predicted by this potential function, are in conformity with a majority of studies cited in the previous section.

In the case of Na^+DMP^- ion pair, sodium–water interactions were computed according to the "simple" model of Clementi and coworkers,[65] the behavior of which was well characterized in an earlier publication[66] from this laboratory. The interaction potential and the geometry for the anionic (DMP^-) part of the ion pair was identical to that described above. Sodium ion was held fixed in the anionic POO^- plane on the bisector of the OPO angle at a distance of 2.21 Å from the anionic oxygens, in conformity with the quantum mechanical calculations of Pack and coworkers[50] on metal-phosphate complexes. This geometry for sodium cation is also in accord with the other theoretical studies quoted in the background section. Partial atomic charges for each conformer of Na^+DMP^- were computed using Gaussian-80 program[63] and basis sets of Clementi and coworkers.[63,67]

In the computer simulations, solute–water interaction was treated under minimum image convention. Intra-solute and inter-solute interactions were not included. Since the solute modeled is never approached by an other solute molecule, the simulated system essentially models infinite dilution. Water–water interactions were truncated at a spherical cutoff of 7.75 Å. Simulations on each conformer involved a total of ca. 3000 K configurations, preceded by 500 K configurations of sampling which were treated as equilibration. The initial configuration was taken from a pre-equilibrated trial run on the appropriate conformation of $[DMP^-]_{aq}$. Ensemble averages for the mean energy are formed over the last 2000 K for each run separately.

We also carried out three additional sets of simulations on $[DMP^-]_{aq}$. The first set involved the anion in identical geometry[13] and charges[30] in all the three conformations. This set, we call fixed geometry calculations, corresponds to the simulations described by Alagona et al. The second set involved all the three conformations in optimized geometry,[22] but with a larger cutoff of 10.5 Å for water–water interactions. The third set involved the anion in optimized geometry, but without density constraints, and corresponds to cluster calculations widely published in the literature. Results of these three sets are quoted selectively.

These calculations were performed on the IBM 3081 machine and each of the 12 simulations on DMP^- with periodic boundary conditions took approximately 100 h of CPU time for the production stage (ca. 2000 K Monte Carlo moves) while the cluster simulations took approximately 50 hours for the same run length.

IV. RESULTS

The calculated internal energies and related quantities for $[DMP^-]_{aq}$ and $[Na^+DMP^-]_{aq}$ are collected in Table I. The quantities entered here are the mean energy $\langle U_{SW} \rangle$ of the system ($N_S = 1$, $N_W = 215$), the energy $\langle U_W \rangle$ of 215 water molecules in $[H_2O]_l$ at 25°C, the corresponding energy $\langle U'_W \rangle$ of solvent water in $[DMP]_{aq}$, the calculated partial molar internal energy of transfer for DMP^- into water, $\langle U_S \rangle$ and finally $\langle U'_S \rangle$ and $\langle U_{rel} \rangle$, the solute–solvent and solvent–solvent contributions to $\langle U_S \rangle$. Each of these is formally defined in equations 1–12 and Figure 4 of a previous publication from this laboratory by Swaminathan et al.[68] The statistical noise levels up to a confidence limit of 95% (2σ) on each of these quantities are also indicated in Table I underneath the corresponding row. The bottom row in Table I gives the calculated conformational energy differences relative to the trans extended form. The hydration energy is seen to favor the *gt* form in the free anion and the trans extended form in the ion pair. The statistical uncertainties in the total internal energies of hydration indicate that *gg* and *gt* conformers are not well differentiated in DMP^-.

The detailed analysis of the results is based on the Proximity Criterion,[69] as reviewed and extended recently in Ref. 70. Tables II to VII summarize the results of the proximity analysis on $[DMP^-]_{aq}$ and $[Na^+DMP^-]_{aq}$ simulations. Column 1 of these tables list the atom or functional group for which the analyses results are presented in the corresponding row. The sequence adopted is first methyl groups, followed by ester oxygens and then

Table I. Monte Carlo mean energy simulation results on $[DMP^-]_{aq}$ and $[Na^+DMP^-]_{aq}$.

	DMP^-(gg)	DMP^-(gt)	DMP^-(tt)	Na^+DMP^-(gg)	Na^+DMP^-(gt)	Na^+DMP^-(tt)
⟨USW⟩	−1859.25	−1864.55	−1854.58	−1839.77	−1822.38	−1853.01
+/−2*SD	5.46	5.36	8.29	10.30	10.15	7.39
⟨US′⟩	−41.47	−31.74	−32.88	−16.31	−14.24	−34.15
+/−2*SD	3.22	1.90	2.45	4.08	2.24	1.87
⟨UW′⟩	−1817.78	−1832.81	−1821.70	−1823.46	−1818.14	−1818.86
+/−2*SD	4.41	5.01	7.92	9.47	9.90	7.15
⟨UW⟩	−1859.75	−1859.75	−1859.75	−1859.75	−1859.75	−1859.75
+/−2*SD	6.45	6.45	6.45	6.45	6.45	6.45
⟨Urel⟩	41.97	26.94	38.05	36.04	51.61	40.89
+/−2*SD	4.71	4.06	4.60	6.93	7.51	3.09
⟨US⟩	0.50	−4.80	5.17	19.73	37.37	6.74
+/−2*SD	5.71	4.48	5.21	8.04	7.84	3.61
Δ⟨US⟩	−4.67	−9.97	0.00	12.99	30.63	0.00
+/−2*SD	2.34	2.66		7.18	6.96	

anionic PO_2^- group (and Na^+ for the ion pair) ending up with sums/averages for the entire molecule. Column 2 (RFS) gives the first shell radius in Å corresponding to the first minimum of the primary radial distribution functions of the relevant atom or functional group. The first shell proximity analyses of the simulations are based on these limits. Column 3 indicates volumes (VFS) in $Å^3$ of the truncated spherical shell of the Voronoi polyhedron associated with the primary region of the solute analysis unit — be it solute atom or functional group. These volumes are generated by Monte Carlo method using a million random points. Column 4 gives the average coordination number $\langle K \rangle$, computed as the average number of water molecules in the volume VFS. This is followed by local solvent densities $\langle K/V \rangle$ in Column 5 in gm/mL. The average first shell solute binding energies ⟨SLTBE⟩ are reported in column 6 in kcal/mol. These represent the net interaction energies of each analysis unit with water molecules in their first shell. The next column gives the average first shell pair interaction energy ⟨SLTPE⟩ computed by dividing the elements in column 6 by those in column 4 for each row. Column 8 indicates the total number of water molecules contained in the Voronoi polyhedron of each analysis unit. The molecular sum for this column adds up to 215; the total number of water molecules in the central cell. Column 9 gives the total solute binding energy in kcal/mol, which adds to $\langle U_S' \rangle$ for the entire molecule. Columns 10 to 12 summarize water properties as modified by the presence of the solute. $\langle KW \rangle$ is the average coordination number of water molecules belonging to the primary region of the atom/functional group. The reference here is to be made to the MCY liquid water value 4.34.[62] ⟨NNWWPE⟩ is the average near neighbor pair interaction energy of water molecules in each primary region. The value to be compared with is −3.01 kcal/mol for MCY water. ⟨BEWWT⟩ is the total pair interaction energy in kcal/mol of all the waters in each Voronoi polyhedron. The corresponding MCY water value is −17.3 kcal/mol.[62] Column 13 gives functional groups for which the averages are reported in the corresponding row.

The RFS value adopted for carbon atoms is 5.3 Å and is 4.2 Å for methyl hydrogens. This is consistent with earlier studies from this laboratory on $[CH_4]_{aq}$.[68] The first shell radial cutoff for ester oxygens is 3.2, slightly less than 3.3 for oxygens in liquid water, while that for anionic oxygens is 3.0. This contraction of the first shell is explicable in terms of the anionic nature or larger negative charge carried by the anionic oxygens. The value of 3.0 for Na^+ conforms to that adopted in the ion-water studies published from this laboratory[66]. These quantities are chosen from the position of the first minimum in the corresponding primary radial distribution function in the proximity analysis.

The volumes VFS can give a quick estimate of the average number of water molecules ex-

pected at liquid densities. Taking the average volume of water molecule in bulk water as 30 Å^3, the average coordination numbers expected for methyl groups is 10, one per ester oxygens, and four for the PO_2^- for *gg* conformer of DMP^-, if the environment were bulk water like. The Voronoi volumes for the methyl groups in the extended conformations (*gt* & *tt*) increase relative to *gg*, while that of anionic oxygens decrease. The total first shell volumes for the entire molecule show a trend of *gg* < *gt* < *tt*. The Voronoi volumes for the ion pair for each conformer are larger than those for the corresponding anion. These volume elements are used in defining local solvent densities and in discussing the transferabilities of coordination numbers for a given atom or functional group in different molecules.

The calculated coordination numbers for DMP^- averaged over the two methyl groups from the detailed simulation analysis are 8.34, 9.68 and 10.02 for *gg*, *gt*, and *tt* conformations respectively; showing a slight conformational trend. The corresponding averages for the ion pair are 8.29, 9.13 and 9.56 for *gg*, *gt* and *tt* conformations and parallel the conformational trend in the hydrated anion. Methyl group coordination is observed to be relatively unperturbed by the presence of counterion for the *gg* conformer. The extended forms however, show a slight decrease compared to their anionic counterparts. The average coordination number for the ester oxygens in *gg* form of DMP^- is 1.00, while that for *gt* and *tt* is 0.76, showing a decrease for *tt* not expected from the volumes of the primary regions. The corresponding averages for the ion pair follow a similar pattern with 0.95 for *gg*, 0.65 for *gt* and 0.63 for *tt*. The average coordination number for PO_2^- group of *gg* conformation of DMP^- is significantly less (4.25) than for the extended conformations (4.88 for *gt* and 4.68 for *tt*). The corresponding coordination number for PO_2^- for the ion pair are, of course, much smaller, due to the presence of the sodium ion in the ion pair. The cation blocks some of the potential sites of hydration of the anionic oxygens. Here again, the average for *gg* is (1.93) less than that of *gt* (2.47) and *tt* (2.60), indicating that statistical noise does not obscure the smaller coordination of PO_2^- of *gg* conformer. Coordination number for sodium cation is close to 5 and is seen to be relatively insensitive to conformational changes. Thus, counting the two anionic oxygens together, sodium ion is heptacoordinated. This is in contrast to the octahedral coordination, with six waters in the first shell, found from the $[Na^+]_{aq}$ simulations[66,67]. This appears to suggest that modifications are brought about in the solvent structure around the cation by the anionic PO_2^- group, but this may be sensitive to the assumed RFS values and the location of the sodium ion.

The total coordination numbers for DMP^- are 22.93 for *gg*, 25.76 for *gt* and 26.23 for *tt*. The corresponding figures for the ion pair are larger overall, with 25.33 for *gg*, 26.87 for *gt* and 27.87 for *tt*. The reduction in PO_2^- group hydration is more than offset by the hydration complement of the cation to the whole molecule. Here again, the conformational trends of *gg* < *gt* < *tt* are noticeable.

Local solvent densities show some interesting trends. Hydrophobic hydration is characterized by a lower density (~10%) relative to the bulk water value in all six DMP (anion and ion pair) experiments. Ester oxygens show conformational sensitivity both for the anion and the ion pair, with a trend of *gg* > *gt* > *tt*. The anionic PO_2^- group indicates a considerable increase over the liquid water value resulting from electrostriction, although the *gg* conformer of DMP^- is somewhat of an exception. The solvent density of 2.05 for the sodium cation is double that of the bulk water value, clearly giving a structural criterion for electrostriction. The molecular averages for the anion are slightly less than that of liquid water, indicating hydrophobic hydration dominates the overall first shell solvent densities. Values for the ion pair are closer to the bulk water value, indicating that hydration of the counterion compensates the effect of hydrophobic hydration on the local solvent densities.

A large contribution to the first shell binding energies of the anion comes from the anionic (PO_2^-) group hydration, followed by hydrophilic (ester oxygens) and hydrophobic (methyl groups) hydration in all three conformations. The first shell energetics of the ion pair is likewise dominated by the anionic, and then the hydrophilic hydrations. The first shell binding energies for the hydrophobic hydration are positive, with the exception of *tt* conformer. Molecular sums for the first shell hydration are close to −100 kcal/mol for

Table II. Proximity Analysis of the Hydration of DMP^{-}(gg).

AT NO	INDEX	TYPE		RFS	VFS	⟨K⟩	⟨K/V⟩	⟨SLTBE⟩	⟨SLTPE⟩	⟨K⟩	⟨SLTBE⟩	⟨KW⟩	⟨NNWWPE⟩	⟨BEWWT⟩	
					FIRST SHELL SOLUTE PROPERTIES					TOTAL SLT PROPS		WATER PROPERTIES RFSW = 3.30 RCE = 7.75 A			
METHYL GROUPS															
1	6	53	C C1	5.3	2.82	0.0	0.0	0.0	0.0	0.0	0.0	0.0	0.0	0.0	
2	7	61	H H1C1	4.2	95.52	2.91	0.91	−12.455	−4.284	22.106	−4.784	4.39	−2.937	−17.297	
3	8	61	H H2C1	4.2	67.98	1.70	0.75	1.605	0.945	12.964	8.209	4.24	−2.989	−17.108	
4	9	54	H H3C1	4.2	125.14	3.40	0.81	5.900	1.735	30.913	20.879	4.27	−3.028	−17.658	
TOTALS FOR FUNCTIONAL GROUP					291.47	8.01	0.82	−4.949	−0.618	65.983	24.305	4.30	−2.990	−17.428	
5	10	53	C C2	5.3	2.81	0.0	0.0	0.0	0.0	0.0	0.0	0.0	0.0	0.0	
6	11	61	H H1C2	4.2	95.43	3.28	1.03	−14.347	−4.378	22.376	−7.789	4.20	−2.995	−16.859	
7	12	61	H H2C2	4.2	68.09	1.92	0.85	3.297	1.713	13.389	9.449	4.21	−3.060	−17.587	
8	13	54	H H3C2	4.2	125.40	3.47	0.83	3.683	1.062	30.408	18.583	4.18	−3.016	−17.244	
TOTALS FOR FUNCTIONAL GROUP					291.73	8.67	0.89	−7.367	−0.850	66.173	20.242	4.19	−3.018	−17.183	
AVERAGES OVER FUNCTIONAL GROUPS: =					291.60	8.34	0.86	−6.158	−0.734	66.078	22.274	4.25	−3.004	−17.306	-CH3
STATISTICAL UNCERTAINTY (+/−2*SD)						0.16	0.02	0.425	0.051	0.02	1.912	0.02	0.056	0.106	
ESTER OXYGENS															
9	4	52	O O3ES	3.2	29.58	1.25	1.27	−13.467	−10.747	6.161	−15.300	4.05	−2.921	−14.780	
10	5	52	O O4ES	3.2	29.54	0.75	0.76	−5.101	−6.830	5.155	−6.048	4.16	−2.909	−16.248	
AVERAGES OVER FUNCTIONAL GROUPS: =					29.56	1.00	1.01	−9.284	−8.788	5.658	−10.674	4.10	−2.915	−15.514	-O-
STATISTICAL UNCERTAINTY (+/−2*SD)						0.06	0.05	1.848	1.764	0.01	3.329	0.06	0.182	0.320	
PO2 GROUP															
11	1	51	P PHOS	5.0	6.22	0.0	0.0	0.0	0.0	0.0	0.0	0.0	0.0	0.0	
12	2	55	O O1AN	3.0	59.42	2.13	1.07	−33.934	−15.932	36.016	−34.323	4.33	−2.866	−16.387	
13	3	55	O O2AN	3.0	59.33	2.12	1.07	−32.233	−15.174	35.512	−30.349	4.30	−2.879	−16.728	
TOTALS FOR FUNCTIONAL GROUP					124.97	4.25	1.02	−66.168	−15.554	71.528	−64.672	4.32	−2.872	−16.557	>P02-
STATISTICAL UNCERTAINTY (+/−2*SD)						0.16	0.04	9.019	2.137	0.03	7.937	0.02	0.071	0.134	
DMP-															
MOLECULAR SUM/AVERAGE:					767.29	22.93	0.89	−97.052	−4.233	215.000	−41.473	4.26	−2.955	−16.957	DMP-
STATISTICAL UNCERTAINTY (+/−2*SD)						0.37	0.01	5.699	0.250	0.04	3.218	0.01	0.043	0.080	

Table III. Proximity Analysis of the Hydration of DMP^-(gt).

AT NO	INDEX	TYPE		RFS	VFS	⟨K⟩	⟨K/V⟩	⟨SLTBE⟩	⟨SLTPE⟩	⟨K⟩	⟨SLTBE⟩	⟨KW⟩	⟨NNWWPE⟩	⟨BEWWT⟩	
					FIRST SHELL SOLUTE PROPERTIES					TOTAL SLT PROPS		WATER PROPERTIES RFSW = 3.30 RCE = 7.75 A			
METHYL GROUPS															
1	6	53	C C1	5.3	2.81	0.0	0.0	0.0	0.0	0.0	0.0	0.0	0.0	0.0	
2	7	61	H H1C1	4.2	97.30	3.20	0.98	−6.868	−2.148	21.083	0.395	4.21	−2.992	−17.012	
3	8	61	H H2C1	4.2	96.26	2.87	0.89	−1.009	−0.351	22.638	6.019	4.23	−3.068	−17.544	
4	9	54	H H3C1	4.2	124.11	3.69	0.89	0.978	0.265	29.291	17.338	4.23	−2.999	−17.395	
TOTALS FOR FUNCTIONAL GROUP					320.47	9.76	0.91	−6.899	−0.707	73.011	23.751	4.23	−3.018	−17.330	
5	10	53	C C2	5.3	2.81	0.0	0.0	0.0	0.0	0.0	0.0	0.0	0.0	0.0	
6	11	61	H H1C2	4.2	85.35	2.44	0.85	−0.762	−0.312	15.600	6.320	4.23	−2.897	−17.015	
7	12	61	H H2C2	4.2	95.48	3.09	0.97	−7.240	−2.346	21.667	1.689	4.26	−3.003	−17.289	
8	13	54	H H3C2	4.2	129.27	4.07	0.94	3.354	0.824	33.495	16.060	4.33	−3.002	−17.960	
TOTALS FOR FUNCTIONAL GROUPS					312.90	9.60	0.92	−4.649	−0.484	70.762	24.069	4.28	−2.979	−17.540	
AVERAGES OVER FUNCTIONAL GROUPS:=					316.69	9.68	0.91	−5.774	−0.596	71.88'7	23.910	4.25	−2.999	−17.435	-CH3
STATISTICAL UNCERTAINTY (+/−2*SD)						0.10	0.02	0.182	0.017	0.03	1.493	0.02	0.032	0.086	
ESTER OXYGENS															
9	4	52	O O3ES	3.2	20.20	0.69	1.02	−5.649	−8.175	1.330	−5.771	3.75	−2.915	−13.160	
10	5	52	O O4ES	3.2	35.13	0.83	0.71	−7.293	−8.759	7.528	−3.930	4.20	−2.895	−16.449	
AVERAGES OVER FUNCTIONAL GROUPS:=					27.66	0.76	0.82	−6.471	−8.467	4.429	−4.851	3.98	−2.905	−14.805	-O-
STATISTICAL UNCERTAINTY (+/−2*SD)						0.05	0.05	0.725	0.877	0.01	1.301	0.06	0.123	0.288	
PO2 GROUP															
11	1	51	P PHOS	5.0	6.26	0.0	0.0	0.0	0.0	0.0	0.0	0.0	0.0	0.0	
12	2	55	O O1AN	3.0	52.21	2.42	1.38	−38.318	−15.859	26.171	−31.800	4.24	−2.888	−16.627	
13	3	55	O O2AN	3.0	60.76	2.46	1.21	−38.585	−15.655	36.197	−38.056	4.22	−2.919	−16.391	
TOTALS FOR FUNCTIONAL GROUP					119.23	4.88	1.22	−76.903	−15.756	62.368	−69.857	4.23	−2.906	−16.490	>PO2
STATISTICAL UNCERTAINTY (+/−2*SD)						0.18	0.04	4.805	0.912	0.03	6.921	0.03	0.046	0.120	
DMP-															
MOLECULAR SUM/AVERAGE					807.93	25.76	0.95	−101.393	−3.936	215.000	−31.738	4.24	−2.968	−17.097	DMP-
STATISTICAL UNCERTAINTY (+/−2*SD)						0.42	0.01	2.761	0.099	0.06	1.903	0.01	0.026	0.068	

Table IV. Proximity Analysis of the Hydration of DMP^- (tt).

AT NO	INDEX	TYPE		RFS	FIRST SHELL SOLUTE PROPERTIES VFS	⟨K⟩	⟨K/V⟩	⟨SLTBE⟩	⟨SLTPE⟩	TOTAL SLT PROPS ⟨K⟩	⟨SLTBE⟩	WATER PROPERTIES RFSW = 3.30 RCE = 7.75 A ⟨KW⟩	⟨NNWWPE⟩	⟨BEWWT⟩	
METHYL GROUPS															
1	6	53	C C1	5.3	2.83	0.0	0.0	0.0	0.0	0.0	0.0	0.0	0.0	0.0	
2	7	61	H H1C1	4.2	97.90	3.01	0.92	−9.063	−3.009	21.278	−2.077	4.25	−3.018	−17.101	
3	8	61	H H2C1	4.2	98.26	3.16	0.96	−0.260	−0.082	21.174	4.838	4.26	−2.987	−17.369	
4	9	54	H H3C1	4.2	129.59	4.07	0.94	1.980	0.487	35.788	17.308	4.25	−2.993	−17.310	
TOTALS FOR FUNCTIONAL GROUP					328.58	10.24	0.93	−7.343	−0.717	78.239	20.069	4.25	−2.998	−17.269	
5	10	53	C C2	5.3	2.83	0.0	0.0	0.0	0.0	0.0	0.0	0.0	0.0	0.0	
6	11	61	H H1C2	4.2	98.26	2.87	0.87	−1.991	−0.695	21.914	5.072	4.25	−2.999	−17.338	
7	12	61	H H2C2	4.2	97.90	2.91	0.89	−5.395	−1.852	22.173	2.248	4.45	−2.975	−17.808	
8	13	54	H H3C2	4.2	129.59	4.02	0.93	−0.599	−0.149	34.033	15.749	4.21	−2.976	−17.133	
TOTALS FOR FUNCTIONAL GROUP					328.58	9.80	0.89	−7.985	−0.815	78.121	23.068	4.29	−2.982	−17.377	
AVERAGES OVER FUNCTIONAL GROUPS:=					328.58	10.02	0.91	−7.664	−0.766	78.180	21.569	4.27	−2.990	−17.323	-CH3
STATISTICAL UNCERTAINTY (+/−2*SD)						0.26	0.02	0.123	0.026	0.02	1.791	0.02	0.027	0.087	
ESTER OXYGENS															
9	4	52	O O3ES	3.2	30.67	0.81	0.79	−7.977	−9.795	3.379	−8.398	4.00	−2.914	−14.436	
10	5	52	O O4ES	3.2	30.67	0.70	0.68	−6.261	−8.951	3.311	−6.725	4.03	−2.858	−14.533	
AVERAGES OVER FUNCTIONAL GROUPS:=					30.67	0.76	0.74	−7.119	−9.373	3.345	−7.561	4.02	−2.886	−14.485	-O-
STATISTICAL UNCERTAINTY (+/−2*SD)						0.07	0.07	0.415	1.179	0.00	3.087	0.07	0.127	0.352	
PO2 GROUP															
11	1	51	P PHOS	5.0	6.03	0.0	0.0	0.0	0.0	0.0	0.0	0.0	0.0	0.0	
12	2	55	O O1AN	3.0	54.25	2.58	1.42	−39.920	−15.500	25.761	−36.105	4.21	−2.955	−16.427	
13	3	55	O O2AN	3.0	54.07	2.10	1.16	−32.803	−15.589	26.189	−24.785	4.31	−2.887	−16.417	
TOTALS FOR FUNCTIONAL GROUP					114.35	4.68	1.22	−72.723	−15.540	51.950	−60.890	4.26	−2.920	−16.422	>PO2-
STATISTICAL UNCERTAINTY (+/−2*SD)						0.25	0.07	2.422	1.111	0.02	8.932	0.03	0.046	0.143	
DMP-															
MOLECULAR SUM/AVERAGE:					832.85	26.23	0.94	−102.290	−3.899	215.000	−32.875	4.26	−2.970	−17.015	DMP-
STATISTICAL UNCERTAINTY (+/−2*SD)						0.59	0.02	1.437	0.118	0.04	2.450	0.01	0.023	0.073	

Table V. Proximity Analysis of the Hydration of Na^+DMP^-(gg).

AT NO	INDEX	TYPE	RFS	VFS	⟨K⟩	⟨K/V⟩	⟨SLTBE⟩	⟨SLTPE⟩	⟨K⟩	⟨SLTBE⟩	⟨KW⟩	⟨NNWWPE⟩	⟨BEWWT⟩
				FIRST SHELL SOLUTE PROPERTIES					TOTAL SLT PROPS		WATER PROPERTIES RFSW = 3.30		RCE = 7.75 A
METHYL GROUPS													
1	6	53 C C1	5.3	2.88	0.0	0.0	0.0	0.0	0.0	0.0	0.0	0.0	0.0
2	7	61 H H1C1	4.2	92.83	2.97	0.96	−3.240	−1.092	22.668	6.781	4.27	−2.947	−17.235
3	8	61 H H2C1	4.2	66.26	1.86	0.84	2.581	1.384	10.990	9.807	4.16	−3.097	−17.472
4	9	54 H H3C1	4.2	121.42	3.53	0.87	5.903	1.672	28.395	16.805	4.18	−3.028	−17.378
TOTALS FOR FUNCTIONAL GROUP				283.39	8.36	0.88	5.244	0.627	62.052	33.393	4.21	−3.010	−17.342
5	10	53 C C2	5.3	2.85	0.0	0.0	0.0	0.0	0.0	0.0	0.0	0.0	0.0
6	11	61 H H1C2	4.2	92.92	2.75	0.89	0.205	0.075	20.454	13.647	4.27	−2.997	−17.677
7	12	61 H H2C2	4.2	66.49	2.01	0.90	3.649	1.816	10.957	9.021	4.13	−3.052	−17.139
8	13	54 H H3C2	4.2	121.84	3.45	0.85	6.081	1.762	30.303	22.378	4.28	−3.020	−17.722
TOTALS FOR FUNCTIONAL GROUP				284.09	8.21	0.86	9.936	1.209	61.714	45.046	4.25	−3.018	−17.603
AVERAGES OVER FUNCTIONAL GROUPS:=				283.74	8.29	0.87	7.590	0.918	61.883	39.219	4.23	−3.014	−17.473 -CH3
STATISTICAL UNCERTAINTY (+/−2*SD)					0.25	0.03	0.332	0.048	0.031	12.924	0.01	0.044	0.148
ESTER OXYGENS													
9	4	52 O O3ES	3.2	28.96	0.95	0.98	−7.316	−7.688	4.448	−5.497	4.14	−2.781	−15.378
10	5	52 O O4ES	3.2	28.95	0.90	0.92	−4.258	−4.757	5.376	−3.902	4.20	−2.879	−15.912
AVERAGES OVER FUNCTIONAL GROUPS:=				28.95	0.92	0.95	−5.787	−6.223	4.912	−4.699	4.17	−2.830	−15.645 -O-
STATISTICAL UNCERTAINTY (+/−2*SD)					0.10	0.10	0.897	1.163	0.009	5.497	0.04	0.146	0.469
PO2 GROUP													
11	1	51 P PHOS	5.0	6.02	0.0	0.0	0.0	0.0	0.0	0.0	0.0	0.0	0.0
12	2	55 O O1AN	3.0	42.87	0.74	0.52	−4.977	−6.699	14.452	−4.982	4.30	−2.941	−16.809
13	3	55 O O2AN	3.0	42.64	1.19	0.83	−9.799	−8.237	14.764	−8.985	4.46	−2.823	−16.888
TOTALS FOR FUNCTIONAL GROUP				91.53	1.93	0.63	−14.776	−7.646	29.216	−13.967	4.38	−2.880	−16.849 >PO2-
STATISTICAL UNCERTAINTY (+/−2*SD)					0.12	0.04	1.329	0.829	0.030	9.473	0.03	0.086	0.293
NA+ CATION													
14	14	2 NA NA+	3.0	72.39	4.97	2.05	−86.957	−17.485	52.194	−71.383	4.39	−2.762	−16.211 NA+
STATISTICAL UNCERTAINTY (+/−2*SD)					0.23	0.10	5.850	1.418	0.040	36.223	0.02	0.062	0.211
DMP-.NA+													
MOLECULAR SUM/AVERAGE:				789.30	25.33	0.96	−98.127	−3.874	215.000	−16.310	4.29	−2.925	−17.000 DMP-.NA+
STATISTICAL UNCERTAINTY (+/−2*SD)					0.57	0.02	3.253	0.155	0.082	4.078	0.01	0.032	0.109

Table VI. Proximity Analysis of the Hydration of Na^+DMP^-(gt).

AT NO	INDEX	TYPE	RFS	VFS	⟨K⟩	⟨K/V⟩	⟨SLTBE⟩	⟨SLTPE⟩	⟨K⟩	⟨SLTBE⟩	⟨KW⟩	⟨NNWWPE⟩	⟨BEWWT⟩	
				FIRST SHELL SOLUTE PROPERTIES					TOTAL SLT PROPS		WATER PROPERTIES RFSW = 3.30		RCE = 7.75 A	
METHYL GROUPS														
1	6	53 C C1	5.3	2.77	0.0	0.0	0.0	0.0	0.0	0.0	0.0	0.0	0.0	
2	7	61 H H1C1	4.2	93.22	2.79	0.89	−2.454	−0.881	20.428	7.816	4.23	−3.017	−17.264	
3	8	61 H H2C1	4.2	83.28	2.21	0.79	3.433	1.556	15.499	13.173	4.11	−3.079	−17.262	
4	9	54 H H3C1	4.2	125.66	4.17	0.99	5.023	1.206	32.102	20.493	4.23	−3.039	−17.215	
TOTALS FOR FUNCTIONAL GROUP				304.93	9.16	0.90	6.002	0.655	68.028	41.482	4.20	−3.041	−17.241	
5	10	53 C C2	5.3	2.79	0.0	0.0	0.0	0.0	0.0	0.0	0.0	0.0	0.0	
6	11	61 H H1C2	4.2	89.69	3.07	1.02	0.347	0.113	17.955	8.711	4.20	−3.134	−17.408	
7	12	61 H H2C2	4.2	91.43	2.48	0.81	−3.424	−1.379	18.126	5.271	4.21	−3.005	−17.131	
8	13	54 H H3C2	4.2	120.58	3.56	0.88	6.089	1.712	26.111	19.410	4.37	−3.036	−17.952	
TOTALS FOR FUNCTIONAL GROUP				304.49	9.11	0.89	3.012	0.331	62.193	33.392	4.27	−3.055	−17.549	
AVERAGES OVER FUNCTIONAL GROUPS:=				304.71	9.13	0.90	4.507	0.493	65.110	37.437	4.24	−3.048	−17.395 -CH3	
STATISTICAL UNCERTAINTY (+/−2*SD)					0.26	0.03	0.134	0.014	0.016	7.572	0.02	0.038	0.073	
ESTER OXYGENS														
9	4	52 O O3ES	3.2	20.04	0.23	0.35	−0.873	−3.726	0.784	−0.473	3.71	−3.101	−15.602	
10	5	52 O O4ES	3.2	34.12	0.95	0.83	−3.879	−4.080	7.762	−1.598	4.14	−2.980	−16.427	
AVERAGES OVER FUNCTIONAL GROUPS:=				27.08	0.59	0.65	−2.376	−3.903	4.273	−1.035	3.93	−3.040	−16.014 -O-	
STATISTICAL UNCERTAINTY (+/−2*SD)					0.07	0.08	0.275	0.422	0.004	0.817	0.07	0.149	0.262	
PO2 GROUP														
11	1	51 P PHOS	5.0	6.10	0.0	0.0	0.0	0.0	0.0	0.0	0.0	0.0	0.0	
12	2	55 O O1AN	3.0	45.52	1.61	1.06	−13.404	−8.334	20.201	−7.699	4.30	−2.905	−16.735	
13	3	55 O O2AN	3.0	36.91	0.86	0.70	−7.463	−8.664	9.261	−6.708	4.41	−2.809	−16.543	
TOTALS FOR FUNCTIONAL GROUP				88.52	2.47	0.83	−20.867	−8.449	29.462	−14.407	4.33	−2.874	−16.674 >PO2-	
STATISTICAL UNCERTAINTY (+/−2*SD)					0.15	0.05	1.300	0.492	0.015	6.126	0.04	0.076	0.147	
NA+ CATION														
14	14	2 NA NA+	3.0	70.38	4.95	2.10	−81.887	−16.543	46.771	−72.633	4.36	−2.686	−15.681 NA+	
STATISTICAL UNCERTAINTY (+/−2*SD)					0.24	0.10	4.049	0.764	0.019	24.512	0.03	0.056	0.110	
DMP-.NA+ MOLECULAR SUM/AVERAGE:				822.48	26.87	0.98	−98.491	−3.666	215.000	−14.235	4.27	−2.941	−16.874 DMP-.NA+	
STATISTICAL UNCERTAINTY (+/−2*SD)					0.60	0.02	2.272	0.079	0.042	2.241	0.01	0.029	0.055	

Table VII. Proximity Analysis of the Hydration of Na^+DMP^-(tt).

AT NO	INDEX	TYPE	RFS	VFS	⟨K⟩	⟨K/V⟩	⟨SLTBE⟩	⟨SLTPE⟩	⟨K⟩	⟨SLTBE⟩	⟨KW⟩	⟨NNWWPE⟩	⟨BEWWT⟩	
				FIRST SHELL SOLUTE PROPERTIES					TOTAL SLT PROPS		WATER PROPERTIES RFSW = 3.30		RCE = 7.75 A	
METHYL GROUPS														
1	6	53 C C1	5.3	2.73	0.0	0.0	0.0	0.0	0.0	0.0	0.0	0.0	0.0	
2	7	61 H HlC1	4.2	92.35	2.62	0.85	−3.342	−1.275	19.638	5.923	4.21	−2.986	−17.082	
3	8	61 H H2C1	4.2	92.16	2.66	0.86	−4.365	−1.641	21.128	4.740	4.28	−2.971	−17.412	
4	9	54 H H3C1	4.2	125.76	4.11	0.98	7.058	1.716	30.692	16.462	4.17	−3.012	−17.435	
TOTALS FOR FUNCTIONAL GROUP				312.99	9.40	0.90	−0.649	−0.069	71.458	27.125	4.21	−2.992	−17.331	
5	10	53 C C2	5.3	2.73	0.0	0.0	0.0	0.0	0.0	0.0	0.0	0.0	0.0	
6	11	61 H HlC2	4.2	92.16	2.73	0.89	−6.053	−2.215	19.302	4.873	4.21	−3.036	−17.255	
7	12	61 H H2C2	4.2	92.35	2.73	0.89	−3.703	−1.355	18.444	6.465	4.21	−3.008	−17.317	
8	13	54 H H3C2	4.2	125.76	4.26	1.01	3.481	0.817	34.556	14.863	4.28	−3.070	−17.905	
TOTALS FOR FUNCTIONAL GROUP				312.99	9.72	0.93	−6.274	−0.645	72.302	26.201	4.25	−3.045	−17.578	
AVERAGES OVER FUNCTIONAL GROUPS:=				312.99	9.56	0.91	−3.462	−0.357	71.880	26.663	4.23	−3.019	−17.454	−CH3
STATISTICAL UNCERTAINTY (+/−2*SD)					0.22	0.02	0.120	0.014	0.026	1.789	0.02	0.027	0.088	
ESTER OXYGENS														
9	4	52 O O3ES	3.2	30.13	0.61	0.61	−3.238	−5.302	3.012	−1.671	3.90	−3.057	−16.134	
10	5	52 O O4ES	3.2	30.13	0.66	0.65	−3.148	−4.783	3.012	−1.267	3.87	−3.010	−15.925	
AVERAGES OVER FUNCTIONAL GROUPS:=				30.13	0.63	0.63	−3.193	−5.042	3.012	−1.469	3.88	−3.033	−16.029	−O−
STATISTICAL UNCERTAINTY (+/−2*SD)					0.07	0.07	0.541	0.984	0.005	0.481	0.09	0.133	0.394	
PO2 GROUP														
11	1	51 P PHOS	5.0	5.96	0.0	0.0	0.0	0.0	0.0	0.0	0.0	0.0	0.0	
12	2	55 O OlAN	3.0	39.66	1.64	1.24	−16.070	−9.782	13.362	−11.198	4.27	−2.842	−16.685	
13	3	55 O O2AN	3.0	39.52	0.96	0.72	−8.922	−9.333	12.355	−6.503	4.22	−2.917	−16.681	
TOTALS FOR FUNCTIONAL GROUP				85.14	2.60	0.91	−24.992	−9.617	25.716	−17.701	4.25	−2.878	−16.683	>PO2−
STATISTICAL UNCERTAINTY (+/−2*SD)					0.14	0.05	2.051	0.909	0.022	2.808	0.05	0.061	0.199	
NA+ CATION														
14	14	2 NA NA+	3.0	69.16	4.89	2.11	−80.738	−16.519	39.499	−66.838	4.34	−2.649	−15.508	NA+
STATISTICAL UNCERTAINTY (+/−2*SD)					0.22	0.09	5.347	1.259	0.027	8.556	0.04	0.045	0.149	
DMP−NA+														
MOLECULAR SUM/AVERAGE:				840.54	27.87	0.99	−119.040	−4.271	215.000	−34.151	4.24	−2.932	−16.962	DMP-.NA+
STATISTICAL UNCERTAINTY (+/−2*SD)					0.53	0.02	3.379	0.140	0.063	1.874	0.02	0.022	0.07	

drophobic groups are much smaller relative to the ionic and hydrophilic groups.

Finally, Table VIII summarizes some pertinent results from the other sets of simulations (columns 2^b to 4^d) on DMP^-. These are compared with the results from the main calculations (column 1^a) reported above. Energies are given in kcal/mol. Partial atomic charges (in atomic units) assumed in different simulations on DMP^- are collected in Table IX.

A larger cutoff (column 2^b) for water–water interactions results in a small, but significant, decrease in interactions originating both in water–water and solute–water terms. Solute binding energies show similar trends as in the main calculations reported above. The differences in the structural aspects are most pronounced for the anionic hydration in the *gg* form. Small changes are noticed for the extended forms. Hydration of methyl groups and ester oxygens and the total coordination numbers show conformational trends mostly matching with the main calculations.

Results on the fixed geometry and charge simulations (column 3^c of Table VIII) show a significant increase in the binding energies relative to the calculations previously described. The interactions are more negative by about 71 kcal/mol for the *gg* conformer, and by ~83 and 81 kcal/mol for *gt* and *tt* conformations, respectively. Given that the geometry for *gg* conformer is more or less similar in both studies, these differences are mainly attributable to the magnitude of charges, and point out the sensitivity of the calculated energetics to reasonable range of choices for these parameters. Optimization of the valence angle is seen to destabilize solute–water interactions, over and above the charge effect, by about 10 kcal/mol. However, the total internal energies of hydration favor the *gg* conformer relative to *gt* in the fixed charge and geometry calculations, while in the optimized geometry calculations the *gg* and *gt* conformers are energetically indistinguishable in consonance with the theoretical studies on DMP^- in vacuum mentioned in the background section. Hydrophobic hydration in the first shell is slightly larger, with coordination numbers per methyl group varying from 9.5 to 10.6. Hydrophobic hydration and the total coordination numbers show similar trends as in the other sets.

Column 4^d of Table VIII reproduces some pertinent results on $[DMP^-]_{aq}$ of Alagona, et al. A comparison of fixed geometry and charge calculations, and that of Alagona, et al. shows that conformational trends match for the over all energetics and water–water interactions. However, their results differ from the main calculations (column 1^a) presented above in that *gt* conformer was found to be more stable with regard to solute–water interactions, while the net conformational preference for *gg* in the total energetics in their calculations, originates in water–water terms, which, as they observed, are more sensitive to statistical noise and convergence aspects of the runs. The total solute–water terms are more negative in their calculations. One major difference in the energy terms between the two sets arises in the water–water interactions which is $-2164.4 +/- 2.3$ kcal/mol for TIPS-4P water and $-1859.75 +/- 6.5$ kcal/mol for MCY water for a system of 215 water molecules. A slightly smaller value for methyl group coordination is obtained in their simulations, which is probably attributable to a smaller radial cutoff of 4.7 used for the first shell in their analysis. Also, in general, the united atom representation relative to a discrete representation is expected to give a smaller coordination number for the same cutoff as the accessible surface area is smaller in the former representation. That *gg* form should have a larger methyl coordination than *gt* is counter-intuitive. This is due either to differences in their analysis procedure, or to the united atom representation for methyl groups used in their simulations. Over seven waters were assigned to PO_4^- group hydration; slightly more than in the present study. This is possibly related to the potential function. The minimum in their potential function for phosphate water interaction (−16.07 kcal/mol) is over 6 kcal/mole higher than that given by the potential function of Clementi and co-workers (−21.6 kcal/mol). A shallower potential energy surface appears to give a larger coordination number. Also, a slightly larger cutoff of 3.2 Å was employed for the anionic oxygens in their analysis.

A visual description of the results on DMP^- (*gt*) cluster calculations is given in Figure 4. Conclusions from cluster calculations appear to be valid for ionic hydration and not for

Table VIII. Energetics and Coordination numbers for $[DMP^-]_{aq}$ from Monte Carlo simulations.

$[DMP^-]_{aq}$		1[a]	2[b]	3[c]	4[d]
Total Energetics					
(g, g)	⟨USW⟩	−1859.3	−1824.6	−1898.4	−2256.8
	⟨US′⟩	−41.5	−33.8	−104.8	−142.7
	⟨UW′⟩	−1817.8	−1790.8	−1793.6	−2114.1
(g, t)	⟨USW⟩	−1864.6	−1821.9	−1878.5	−2228.9
	⟨US′⟩	−31.7	−21.2	−103.8	−147.3
	⟨UW′⟩	−1832.9	−1800.7	−1774.7	−2081.6
(t, t)	⟨USW⟩	−1854.6	−1818.0	−1895.7	—
	⟨US′⟩	−32.9	−21.9	−103.0	—
	⟨UW′⟩	−1821.7	−1796.1	−1792.7	—
First Shell Energetics					
(g, g)	⟨US′(FS)⟩	−97.1	−95.9	−116.5	−88.4
	(>PO2−)	−66.2	−77.3	−79.1	−63.0
	2(−O−)	−18.6	−19.2	−15.6	−8.7
	2(−CH3)	−12.3	+0.6	−21.8	−16.7
(g, t)	⟨US′(FS)⟩	−101.4	−95.2	−116.7	−95.8
	(>PO2−)	−76.9	−83.5	−93.2	−69.7
	2(−O−)	−12.9	−12.9	−9.3	−8.2.
	2(−CH3)	−11.6	+1.2	−9.2	−17.9
(t, t)	⟨US′(FS)⟩	−102.3	−97.7	−124.1	—
	(>PO2−)	−72.7	−75.1	−70.1	—
	2(−O−)	−14.2	−12.4	−17.0	—
	2(−CH3)	−15.4	−10.2	−37.0	—
Coordination Numbers					
(g, g)	Total	22.93	25.42	25.85	22.96
	(>PO2−)	4.25	5.20	5.40	5.61
	2(−O−)	2.00	2.02	1.41	1.47
	2(−CH3)	16.68	18.20	19.04	15.88
(g, t)	Total	25.76	26.41	26.67	22.62
	(>PO2−)	4.88	5.45	5.23	6.00
	2(−O−)	1.52	1.48	1.41	1.53
	2(−CH3)	19.36	19.48	20.03	15.09
(t, t)	Total	26.24	26.26	27.51	—
	(>PO2−)	4.68	4.81	4.58	—
	2(−O−)	1.52	1.11	1.73	—
	2(−CH3)	20.04	20.34	21.19	—

[a]Main Calculations described in the text.
[b]Calculations with a larger cutoff for E(W−W)
[c]Calculations with identical charges and O—P—O valence angle for gg, gt & tt.
[d]From Ref. 40.

hydrophobic hydration—a reasonable expectation since the former is dominated by local solute–solvent interactions, whereas the latter depends on the solute volume and solvent–solvent interactions.

V. DISCUSSION

The essential structural features of the aqueous hydration of the dimethylphosphate anion as described by our simulations is a first hydration shell consisting of 23–26 water molecules, with ~six of the first shell waters identified with hydration of the phosphodiester (PO_4^-) group, and 17–20 with the hydrophobic hydration of the methyl groups. Conformational differences in the PO_4^- hydration show up mainly in a distribution of the six waters among the anionic and ester oxygens. Methyl groups in the *gg* form correspond to a contact pair (C to C distance ~ 3.6 Å) and are expected to be less solvated than in the extended conformations. This is borne out by the simulation results. Counterion admits five additional waters into the first shell of the molecule, while mostly de-

Table IX. Partial Atomic Charges on DMP^- used in the computer simulations.

Atom	DMP^-(gg)	DMP^-(gt)	DMP^-(tt)	DMP^- [a]	DMP^- [b]
P	1.861	1.861	1.857	1.791	0.912
O1	−0.897	−0.905	−0.898	−0.878	−0.655
O2	−0.897	−0.892	−0.898	−0.878	−0.655
O3	−0.621	−0.619	−0.619	−0.631	−0.410
O4	−0.621	−0.631	−0.619	−0.631	−0.410
C1	−0.428	−0.424	−0.424	−0.211	—
H1C1	0.162	0.176	0.174	0.104	—
H2C1	0.165	0.178	0.174	0.104	—
H3C1	0.188	0.164	0.165	0.117	—
C2	−0.428	−0.426	−0.424	−0.211	—
H1C2	0.162	0.180	0.174	0.104	—
H2C2	0.165	0.175	0.174	0.104	—
H3C2	0.188	0.163	0.165	0.117	—
CH3 (1)	0.088	0.095	0.089	0.114	0.109
CH3 (2)	0.088	0.091	0.089	0.114	0.109
DMP^-	−1.000	−1.000	−1.000	−1.000	−1.000

[a] Calculations with identical charges and O—P—O valence angle for gg, gt & tt.
[b] From Ref. 40.

creasing the anionic hydration by about two waters in all conformations, as well as of other functional groups to a minor extent. The hydrophobic hydration, taking into account the accessible volumes, is seen to be unperturbed by the presence of counterion.

Coordination numbers for methyl groups vary from 8–10 in all these simulations and show a high degree of transferability when these are normalized with the accessible first shell volumes. Local solvent densities for the methyl groups in the fully extended form (*tt*), for instance, are 0.91 for the anion and 0.91 for the ion pair, while for *gt*, they are 0.91 for the anion and 0.90 for the ion pair. This agrees with the results on N-methyl acetamide[72] for hydrophobic hydration where methyl groups were assigned 8–9 waters and the results were observed to be independent of the potential functions. PO_4^- group hydration in the anion shows a small scatter, while $Na^+PO_4^-$ group results indicate that the coordination numbers are transferable again.

Local solvent densities of ester oxygens clearly show a conformational effect, with ester oxygens in the *gg* form having a larger

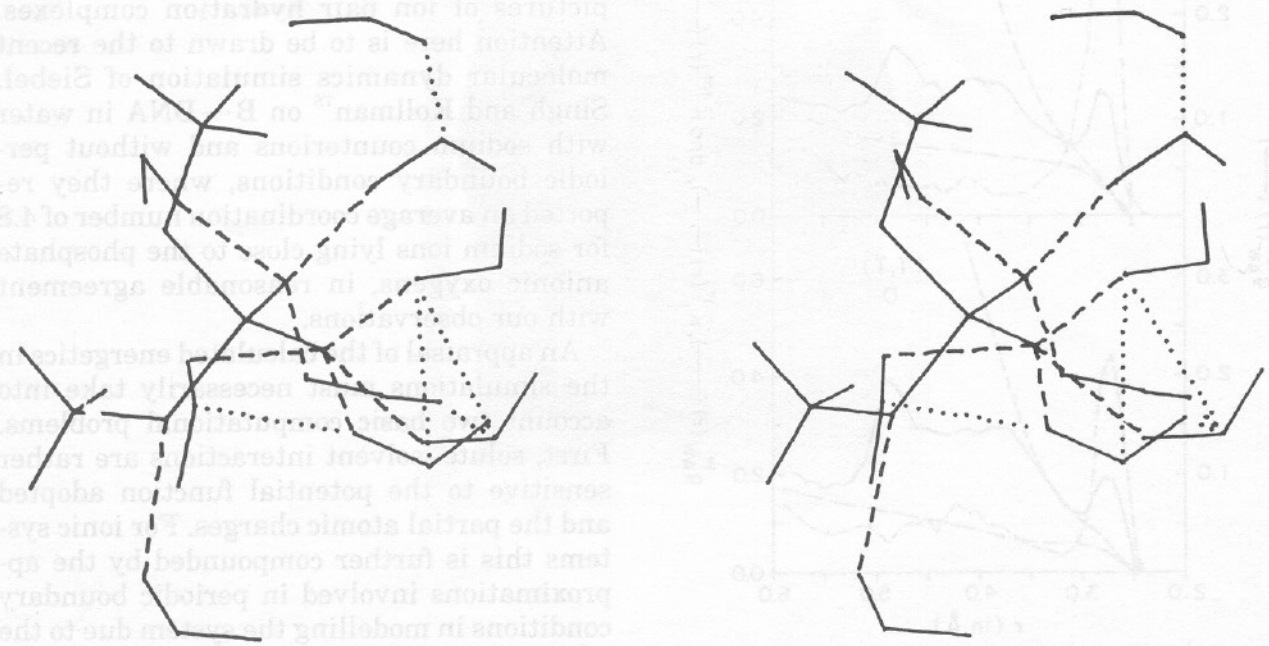

Figure 4. Representative hydration complex emerging from the simulation on $DMP^-(g,t)$-water cluster. Dashes and dots correspond to solute–water (<3.2 Å) and water–water (<3.3 Å) bonds.

value. Figure 5 illustrates this effect. This is akin to the results reported by Pratt and Chandler (Figure 4)[73] on the hydration of butane where the interior methylene sites in the gauche form showed a larger density than the trans methylenes.

Bridged structures are a common theme in theoretical studies on monohydrate complexes as pointed out in the background section. We have looked at the statistical significance of such structures in $[DMP^-]_{aq}$ simulations. Statistical weight of configurations with a bridging water molecule between the two anionic oxygens of the phosphate group is defined as equivalent to the conditional probability for locating a water molecule at a distance of 3.0 Å (first minimum in the radial distribution functions) from both the anionic oxygens. The value obtained for the statistical weight was 0.005, indicating a low probability for such structures in the statistical state of the systems. This observation matches with earlier studies on glycine zwitterion hydration reported from this laboratory[74].

Representative structures illustrating the DMP^- hydration for the *gg*, *gt* and *tt* isomers are shown in Figures 6–8, respectively, and

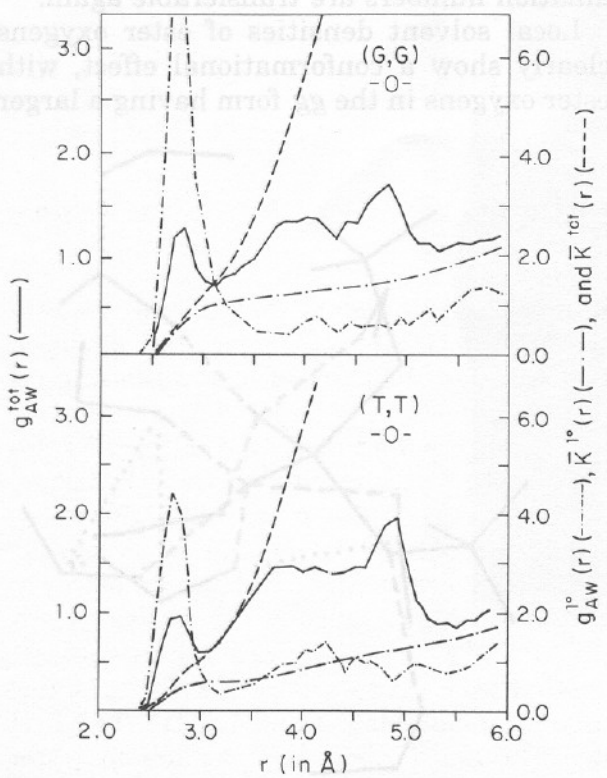

Figure 5. Primary and total radial distribution functions and running coordination numbers of *gg* and *tt* ester oxygens illustrating conformational effect.

for the ion pair in Figures 9–11. Of course, no single structure is representative of an entire simulation, but considered alongside the statistical description of the system given in the preceding section, general features can be considered. The anionic hydration of DMP^- involves primarily sequential, two-center hydrogen bonds in the structures shown. The most common type of interactions in the structures is bent hydrogen bonds. The general organization of the anionic hydration of DMP^- as determined from the simulation clearly reflects the idea of circular zones of hydration predicted in the studies of Pullman and co-workers described above[31,32]. The hydrophilic hydration of DMP^-, essentially one water per ester oxygen, shows an average separation of 2.7 Å, very near the liquid water value. The hydrophobic hydration, quite extensive in DMP^-, is generally as expected; a structure of the hydrophobic hydration shells dominated by water–water than solute–water interactions is shown quite clearly in Figures 6–8. The presence of counterion is seen to increase the number of water–water hydrogen bonds in Figures 9–11. No water molecule is bound to both the sodium ion and the phosphate anionic oxygens simultaneously. Treating the midpoint of the anionic oxygens and the oxygens of water molecules as coordination sites, the symmetry of sodium hydration shell roughly corresponds to an octahedron in all the stereo pictures of ion pair hydration complexes. Attention here is to be drawn to the recent molecular dynamics simulation of Siebel, Singh and Kollman[75] on B—DNA in water with sodium counterions and without periodic boundary conditions, where they reported an average coordination number of 4.8 for sodium ions lying close to the phosphate anionic oxygens, in reasonable agreement with our observations.

An appraisal of the calculated energetics in the simulations must necessarily take into account two basic computational problems. First, solute–solvent interactions are rather sensitive to the potential function adopted and the partial atomic charges. For ionic systems this is further compounded by the approximations involved in periodic boundary conditions in modelling the system due to the long range interactions. Furthermore, a non-negligible contribution for highly charged systems is expected to come from waters be-

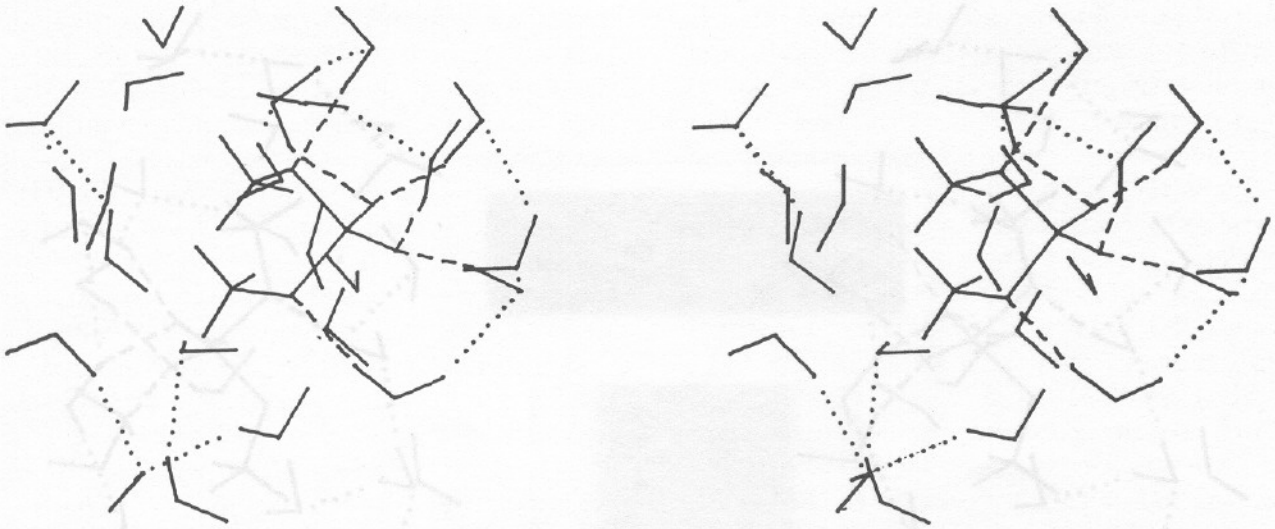

Figure 6. Stereo view of a representative hydration complex of $[DMP^-(g,g)]_{aq}$ sampled from the Monte Carlo run. Dashes and dots have the same significance as in Fig. 4.

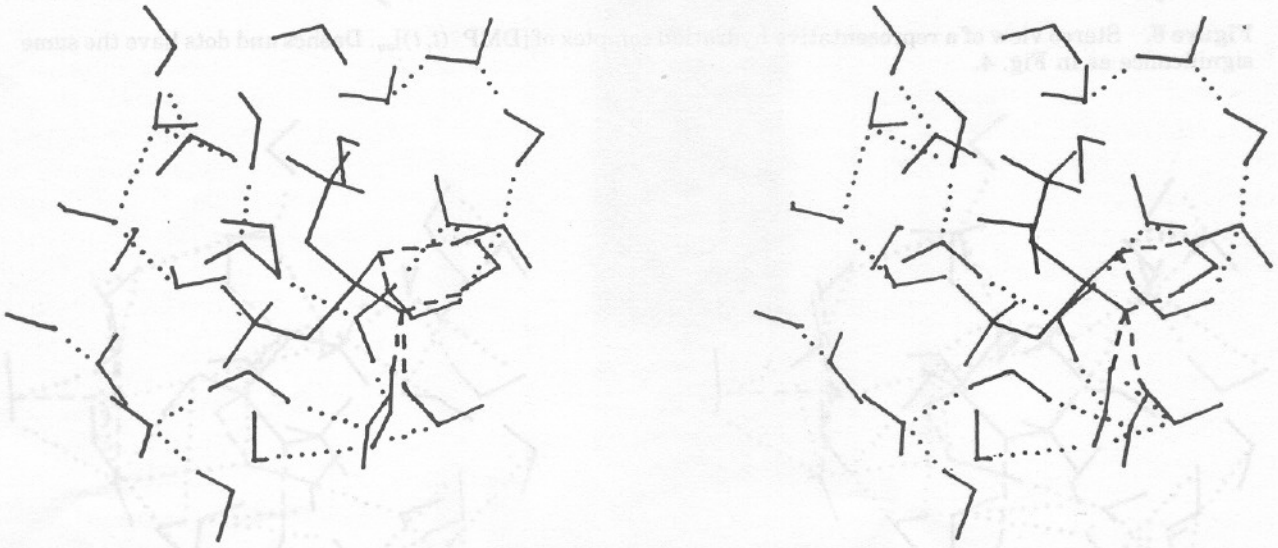

Figure 7. Stereo view of a representative hydration complex of $[DMP^-(g,t)]_{aq}$. Dashes and dots have the same significance as in Fig. 4.

yond the first shell which are numerous. This leads to apprehensions about the small system size in the simulations. Second, solvent–solvent interactions are generally subject to considerable statistical uncertainty despite the long run lengths—more so for ionic systems. These, together with concerns about intermolecular potentials, lead us to only a provisional understanding of the relative stability of various conformations.

Trends in total solute–water interactions parallel conclusions from the continuum model calculations [33], with the *gg* conformer for the anion and *tt* for the ion pair favored over and above the calculated error bounds. The conformational differences in the total internal energies of hydration are not sufficiently significant for an unequivocal interpretation. However, subject to the stated uncertainties, the *tt* conformer of the anion is seen to be destabilized by hydration relative to *gg* and *gt*, whereas it is stabilized by hydration when paired with sodium counterion.

Experimental data on the enthalpies of hydration of DMP^- is not available. Calculated transfer energies of hydration are mostly endothermic. An analysis of the transfer energies for DMP^- (g,g) is presented in Table X, together with the results of (T,P,N) ensemble calculations of Alagona, et al. [40]. The first row of Table X gives the vacuum to water transfer energies $\langle U_S \rangle$. The second and third rows are the water–water $\langle U_{rel} \rangle$, and solute–water $\langle U'_S \rangle$ contributions to the trans-

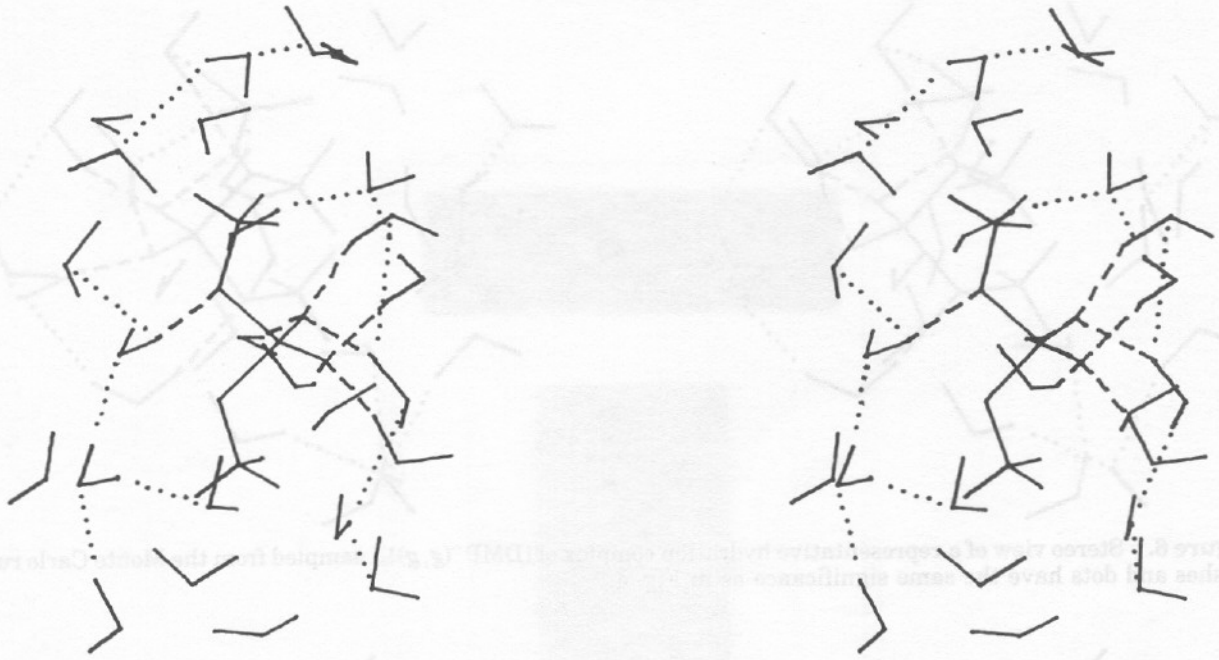

Figure 8. Stereo view of a representative hydration complex of $[DMP^-(t,t)]_{aq}$. Dashes and dots have the same significance as in Fig. 4.

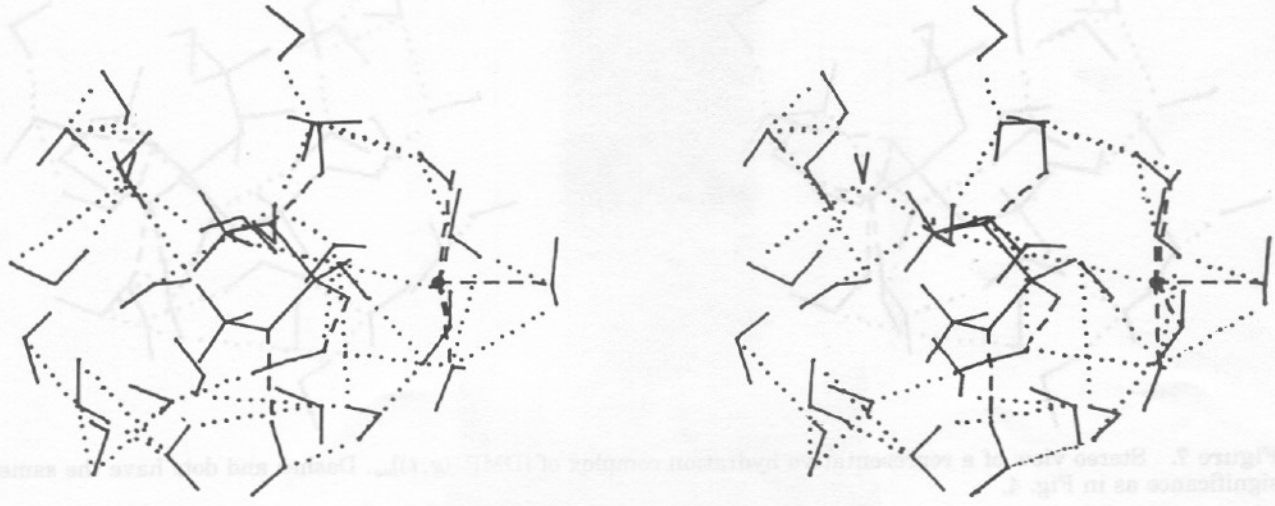

Figure 9. Stereo view of a representative hydration complex of $[Na^+DMP^-(g,g)]_{aq}$. Dashes and dots have the same significance as in Fig. 4.

Table X. Calculated Contributions to the Transfer Energies of DMP^-(gg).

	DMP^-(gg)	DMP^-(gg)[a]
⟨US⟩	0.5	−92.4
⟨Urel⟩	+42.0	+50.3
⟨US′⟩	−41.5	−142.7
⟨US′(FS)⟩	−97.1	−88.4
⟨US′(EXT)⟩	+55.6	−54.3
>PO2−(EXT)	+1.5	—
2(−O−)(EXT)	−3.8	—
2(−CH3)(EXT)	+56.9	—

[a]From Ref. 40.

fer energies, respectively. The $\langle U_{rel} \rangle$ results suggest that, in both cases, DMP^- disrupts the water–water interactions. A similar observation was made earlier with the halide anions and alkali metal cations [66]. The solute–water interactions, however, are much too small in magnitude in the present calculations relative to the results on ion–water simulations ($\langle U_S' \rangle \geq -150$ kcal/mol) of Ref. 66 and of Alagona, et al. These are further analyzed in terms of first shell contributions $\langle U_S'(\text{FS}) \rangle$ given in row 4, and interactions of solute with waters external to the first shell $\langle U_S'(\text{EXT}) \rangle$, given in row 5 (and divided into the constituent func-

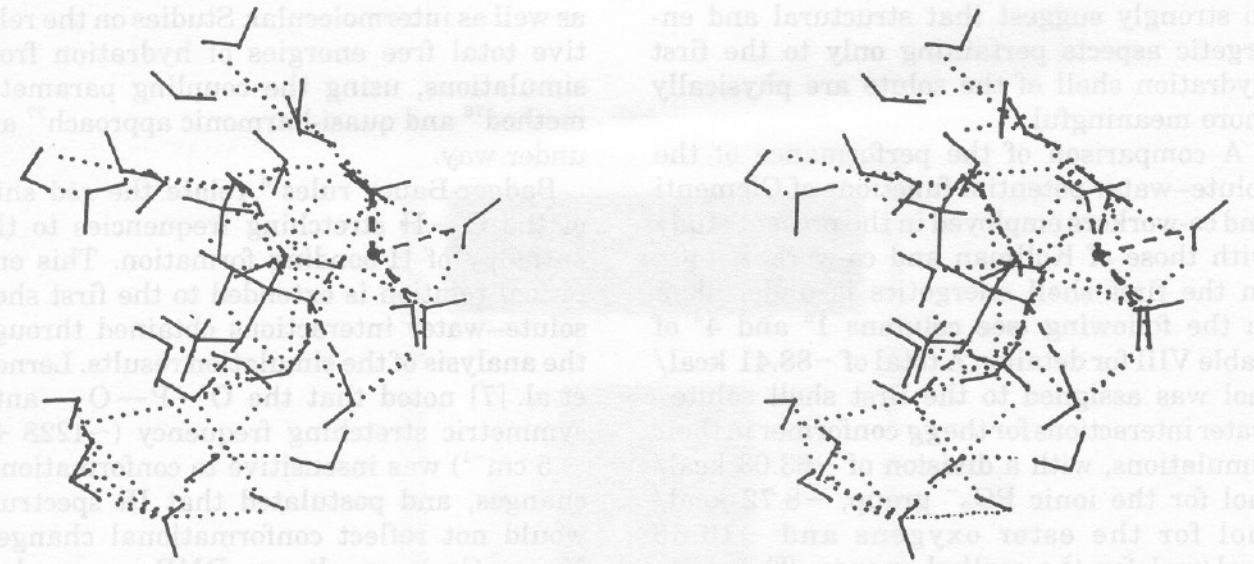

Figure 10. Stereo view of a representative hydration complex of $[Na^+DMP^-(g,t)]_{aq}$. Dashes and dots have the same significance as in Fig. 4.

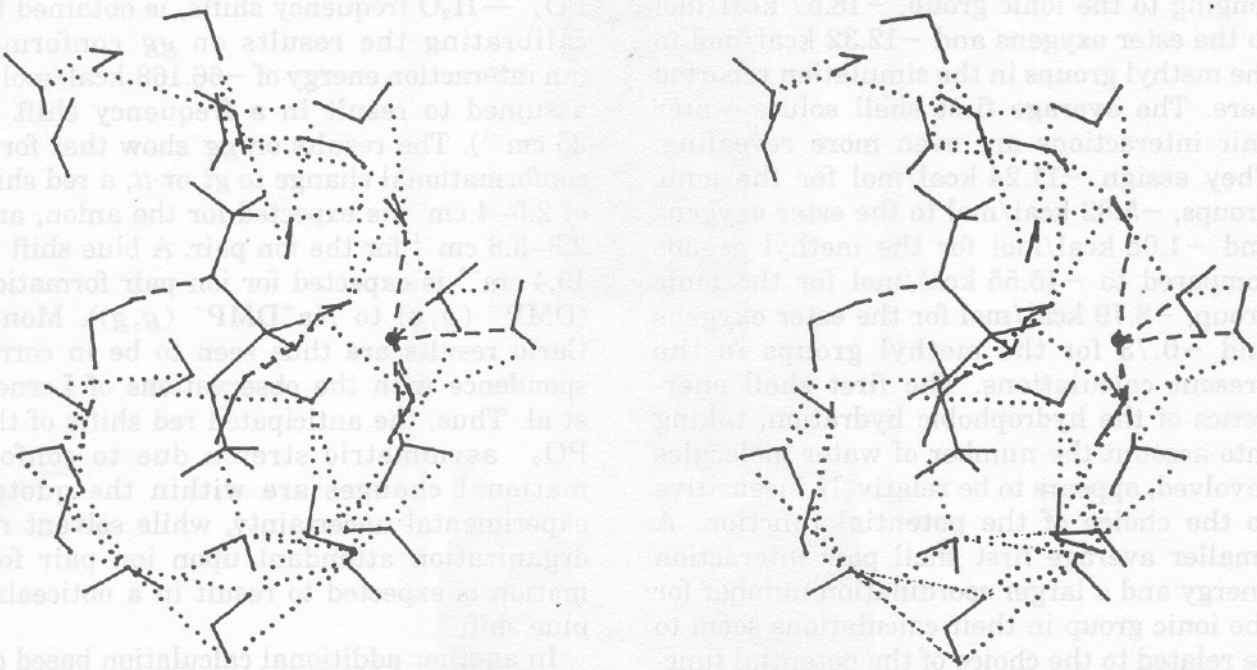

Figure 11. Stereo view of representative hydration complex of $[Na^+DMP^-(t,t)]_{aq}$. Dashes and dots have the same significance as in Fig. 4.

tional group contributions in rows 6, 7 and 8). A contribution of +55.6 kcal/mol for solute–water binding energy from $\langle U'_S(\mathrm{EXT})\rangle$, almost entirely coming from waters proximal to the methyl groups, is clearly unrealistic. Similar symptoms are observed with the *gt* and *tt* conformations of the anion and with the ion pair. Fixed charge and geometry calculations indicate the sensitivity of the solute–water binding energies ($\langle U'_S\rangle$ = −104.8 kcal/mol given in column 3[c] of Table VIII, as opposed to −41.5 kcal/mol in Table X discussed above) and hence, the transfer energies to the choice of partial atomic charges adopted in the simulations as pointed out earlier. While a judicious choice of the solute–water and water–water potential functions is imperative to obtain acceptable transfer energies, another possible source for this discrepancy is modelling the ionic systems through periodic boundary conditions as mentioned earlier. These constitute some, as yet, unresolved methodological issues and further work is needed in this area. The $[DMP^-]_{aq}$ simulation results here (a perusal of Table VIII should suffice) appear

to strongly suggest that structural and energetic aspects pertaining only to the first hydration shell of the solute are physically more meaningful.

A comparison of the performance of the solute–water potential functions of Clementi and co-workers employed in the present study with those of Kollman and co-workers [40], on the first shell energetics is undertaken in the following (see columns 1[a] and 4[d] of Table VIII for details). A total of −88.41 kcal/mol was assigned to the first shell solute–water interactions for the *gg* conformer in their simulations, with a division of −63.03 kcal/mol for the ionic PO_2^- group, −8.72 kcal/mol for the ester oxygens and −16.66 kcal/mol for the methyl groups. This is to be contrasted with a total of −97.05 kcal/mol apportioned as −66.17 kcal/mol belonging to the ionic group, −18.57 kcal/mol to the ester oxygens and −12.32 kcal/mol to the methyl groups in the simulation reported here. The average first shell solute–water pair interactions are even more revealing. They assign −11.24 kcal/mol for the ionic groups, −5.82 kcal/mol to the ester oxygens and −1.05 kcal/mol for the methyl groups compared to −15.55 kcal/mol for the ionic group, −8.79 kcal/mol for the ester oxygens and −0.73 for the methyl groups in the present calculations. The first shell energetics of the hydrophobic hydration, taking into account the number of water molecules involved, appears to be relatively insensitive to the choice of the potential function. A smaller average first shell pair interaction energy and a larger coordination number for the ionic group in their calculations seem to be related to the choice of the potential function, while their product giving the total first shell binding energies cited above for the two potential functions agree well within the statistical uncertainties. Results on the *gt* conformer follow a similar pattern, with the potential function of Clementi and co-workers adopted in the present calculations turning in a slightly more negative term for the average pair interaction energies, and a smaller coordination number for the PO_4^- first shell hydration compared to that of Kollman and co-workers.

The question of relative stability of the various conformers of DMP^- is, of course, a matter of free energy, and involves intramolecular energy and entropy contributions as well as intermolecular. Studies on the relative total free energies of hydration from simulations, using the coupling parameter method[76] and quasi-harmonic approach[77] are under way.

Badger-Bauer rules[78] relate the red shift of the O—H stretching frequencies to the enthalpy of H-bonding formation. This empirical relation is extended to the first shell solute–water interactions obtained through the analysis of the simulation results. Lerner, et al. [7] noted that the O—P—O— antisymmetric stretching frequency (~1228 +/− 5 cm^{-1}) was insensitive to conformational changes, and postulated that IR spectrum would not reflect conformational changes. Monte Carlo results on DMP are used to check this hypothesis through Badger-Bauer rule. The proportionality constant for PO_2^-—H_2O frequency shifts, is obtained by calibrating the results on *gg* conformer (an interaction energy of −66.168 kcal/mol is assumed to result in a frequency shift of 25 cm^{-1}). The results on *gg* show that for a conformational change to *gt* or *tt*, a red shift of 2.5–4 cm^{-1} is expected for the anion, and 2.3–3.8 cm^{-1} for the ion pair. A blue shift of 19.4 cm^{-1} is expected for ion pair formation (DMP^- (g,g) to Na^+DMP^- (g,g)). Monte Carlo results are thus seen to be in correspondence with the observations of Lerner, et al. Thus, the anticipated red shifts of the PO_2^- asymmetric stretch due to conformational changes are within the quoted experimental uncertainty, while solvent reorganization attendant upon ion pair formation is expected to result in a noticeable blue shift.

In another additional calculation based on the simulation results, ^{31}P spin lattice relaxation times of DMP^- in water are estimated following the methodology developed by Hertz and Raedle[79].

$$(1/T_1)_i = 4/3\ \gamma_i^2 \gamma_j^2 \hbar^2 S_j(S_j + 1) \cdot \int \exp(-t/t_c)\, dt \int (g(r)/r^6) 4\pi r^2\, dr\,.$$

The procedure essentially assumes that dipole–dipole (*dd*) relaxation is the dominant mechanism and involves a Markovian approximation for the relaxation process. The appropriate time correlation function[80] then has an exponential decay with rotational correlation time t_c of water as an input parameter (taken from Ref. 81). This is the well

known rapid modulation limit where the solvent motions are on a much shorter time scale relative to the solute motions. The orientationally averaged spatial correlation function then involves evaluation of the ensemble average of $1/r^6$ where r is the distance between the relaxing solute nucleus and the solvent protons. This is evaluated using the radial distribution functions, $g(r_{P-H})$, obtained from the Monte Carlo calculations. The calculated T_1 values for DMP^- are 216.2 seconds, 216.4 seconds and 217.5 seconds for *gg*, *gt* and *tt* conformations, respectively. The experimentally estimated values [45] are close to 20 seconds. Thus, either the procedure is limited in accuracy, or dipole–dipole relaxation is not the dominant mechanism. Shindo[82] finds this as a usual situation met in the case of ^{31}P studies in macromolecules where chemical shift anisotropy provides an efficient alternative means. Conversely, within the *dd* approximation, one can utilize the experimental T_1 values to estimate the rotational correlation times of water in the vicinity of the solute, and comment upon the strength of solute–water interactions computed via the given potential function. For DMP^- the t_c estimate is $\sim 2.5 \times 10^{-11}$ secs, which is probably 3 to 4 times too large for an anion. Thus, the solute–water potential function of Clementi and co-workers [30] employed in the present study appears to over estimate the interactions, or in other words, the first shell water molecules are predicted to be more tightly bound to the solute than is found experimentally.

VI. CONCLUSIONS

To sum up, the phosphodiester group was characterized by a little over six water molecules in its first hydration shell. The total average internal energies of hydration and the relative transfer energies indicated that hydration destabilized the *tt* conformer of the anion, and this mostly originated in the PO_2^- group hydration. Solute–water interactions, in particular phosphate group hydration, favored the *gg* form, and water–water interactions favored the *gt* conformer of the anion. For the ion pair the total average internal energy of hydration was seen to stabilize the fully extended *tt* conformer. Convergence in water–water interactions was noted to be slow in all these simulations. The computed error bounds on the calculated energetics suggested that statistical noise was larger for the ion pair relative to the anion.

A comparison of the solute–water potential functions of Clementi and co-workers, with those of Kollman and co-workers, suggested that a meaningful comparison could be made only for the first shell properties of the solute, wherein the results indicated a number of similarities. A larger cutoff for water–water interactions while preserving the conformational trends in coordination numbers resulted in an increase in the local solvent density of the anion in *gg* conformation. Identical partial atomic charges in all conformations were observed to render the solute–water interactions conformationally indistinguishable. Also, the transfer energies were noticed to be sensitive to the selection of partial atomic charges on the solute. The structural trends in hydration, however, were in general agreement with other sets of simulations.

Preliminary results on the free energies of hydration, as well as relative intramolecular free energies indicated a trend of $gg > gt > tt$ for the stability of the dimethylphosphate anion in water. These are under further investigation.

This research was supported by NIH grant GM 24914 and by NSF grant CHE-8203501.

References

1. W. Saenger, *Principles of Nucleic Acid Structure*, Springer Verlag, New York, 1984.
2. L. Giarda, F. Garbassi and M. Calcaterra, *Acta. Cryst.*, **B29,** 1826 (1973).
3. S. J. Weiner, P. A. Kollman, D. Case, U. C. Singh, C. Ghio, G. Alagona and P. Weiner, *J. Am. Chem. Soc.*, **106,** 765 (1984).
4. T. Shimanouchi, M. Tsuboi and Y. Kyogoku, *Adv. Chem. Phys.*, **7,** 435 (1964).
5. C. Garrigou-Lagrange, O. Bouloussa and C. Clement, *Can. J. Spect.*, **21,** 75 (1976).
6. D. O. Gorenstein, J. B. Findlay, R. K. Momii, B. A. Luxon and D. Kar, *Biochemistry,* **5,** 3796 (1976).
7. D. B. Lerner, W. J. Becktel, R. Everett, M. Goodman and D. R. Kearns, *Biopolymers,* **23,** 2157 (1984).
8. W. K. Olson and P. J. Flory, *Biopolymers,* **11,** 1 (1972).
9. N. Yathindra and M. Sundaralingam, *Proc. Nat. Acad. Sci. USA,* **71,** 3325 (1974).
10. V. Sasisekharan and A. V. Lakshminarayanan, *Biopolymers,* **8,** 505 (1969).
11. A. Saran and G. Govil, *J. Theor. Biol.,* **33,** 407 (1971).
12. A. Pullman, *Biophys. Biochim. Acta,* **269,** 1 (1972).
13. M. D. Newton, *J. Am. Chem. Soc.,* **95,** 256 (1973).
14. G. Govil, *Biopolymers,* **15,** 2303 (1976).

15. G. Lipari and C. Tosi, *Theoret. Chim. Acta (Berl.),* **50,** 169 (1978).
16. A.R. Srinivasan, N. Yathindra, V.S.R. Rao and S. Prakash, *Biopolymers,* **19,** 165 (1980).
17. E. Platt, B. Robson and I. H. Hillier, *J. Theor. Biol.,* **88,** 33 (1981).
18. D. Perahia, B. Pullman and A. Saran, *Biochim. Biophys. Acta,* **340,** 299 (1974).
19. D. Perahia and B. Pullman, *Biochim. Biophys. Acta,* **435,** 282 (1976).
20. D.G. Gorenstein, D. Kar, B.A. Luxon and R.K. Momii, *J. Am. Chem. Soc.,* **98,** 1668 (1976).
21. D.G. Gorenstein and D. Kar, *J. Am. Chem. Soc.,* **99,** 672 (1977).
22. D.G. Gorenstein, B.A. Luxon and J.B. Findlay, *Biochim. Biophys. Acta,* **475,** 184 (1977).
23. H. Berthod and A. Pullman, *Chem. Phys. Lett.,* **32,** 233 (1975).
24. D. Perahia, A. Pullman and H. Berthod, *Theoret. Chim. Acta (Berl.),* **40,** 47 (1975).
25. H. Frischleder,, S. Gleichmann and R. Krohl, *Chem. Phys. Lipids,* **19,** 144 (1977).
26. R. Gay and G. Vanderkooi, *J. Chem. Phys.,* **75,** 2281 (1981).
27. G. Alagona, C. Ghio and P.A. Kollman, *J. Am. Chem. Soc.,* **105,** 5226 (1983).
28. A. Pullman, H. Berthod and N. Gresh, *Chem. Phys. Lett.,* **33,** 11 (1975).
29. G. Corongiu and E. Clementi, *Gazz. Chim. Italiana,* **108,** 687 (1978).
30. E. Clementi, G. Gorongui and F. Lelj, *J. Chem. Phys.,* **70,** 3726 (1979).
31. B. Pullman, A. Pullman, H. Berthod and N. Gresh, *Theoret. Chim. Acta (Berl.),* **40,** 93 (1975).
32. J. Langlet, P. Claverie, B. Pullman and D. Piazzola, *Int. J. Quant. Chem., Quant. Biol. Symp.,* **6,** 409 (1979).
33. T. Bleha, J. Mlynek and I. Tvaroska, *Collection Czech. Chem. Commun.,* **46,** 1722 (1981).
34. K.D. Gibson and H.A. Scheraga, *Proc. Nat. Acad. Sci. USA,* **58,** 420 (1967).
35. L.G. Dunfield, A.W. Burgess and H.A. Scheraga, *J. Phys. Chem.,* **82,** 2601 (1978).
36. Z.I. Hodes, G. Nemethy and H.A. Scheraga, *Biopolymers,* **18,** 1565 (1979).
37. A.J. Hopfinger, *Conformational Properties of Macromolecules,* Acad. Press, New York, 1973, p. 70.
38. A.J. Hopfinger, *Intermolecular Interactions and Biomolecular Organization,* Wiley Interscience, New York, 1977, p. 324.
39. D.L. Beveridge, P.V. Maye, B. Jayaram, G. Ravishanker and M. Mezei, *J. Biomol. Struc. and Dynam.,* **2,** 261 (1984).
40. G. Alagona, C. Ghio and P.A. Kollman, *J. Am. Chem. Soc.,* **107,** 2229 (1985).
41. N.C. Seeman, J.M. Rosenberg, F.L. Suddath, J.J.P. Kim and A. Rich, *J. Mol. Biol.,* **104,** 109 (1976).
42. J.M. Rosenberg, N.C. Seeman, R.O. Day and A. Rich, *J. Mol. Biol.,* **104,** 145 (1976).
43. Y. Kyogoku and Y. Iitaka, *Acta Cryst.,* **21,** 49 (1966).
44. J.P. Hazel, R.L. Collin, *Acta Cryst.,* **B28,** 2951 (1972).
45. T. Glonek and J.R. Van Wazer, *J. Phys. Chem.,* **80,** 639 (1976).
46. R.K. Nanda and G. Govil, *Theoret. Chim. Acta (Berl.),* **38,** 71 (1975).
47. B. Pullman, N. Gresh and H. Berthod, *Theoret. Chim. Acta (Berl.),* **40,** 71 (1975).
48. D.S. Marynick and H.F. Schaefer III, *Proc. Nat. Acad. Sci. USA,* **72,** 3794 (1975).
49. A. Pullman and H. Berthod, *Chem. Phys. Lett.,* **41,** 205 (1976).
50. P. Liebmann, G. Loew, A.D. McLean and G.R. Pack, *J. Am. Chem. Soc.,* **104,** 691 (1982).
51. H. Berthod and A. Pullman, *Chem. Phys. Lett.,* **46,** 249 (1977).
52. A. Pullman, B. Pullman and H. Berthod, *Theoret. Chim. Acta (Berl.),* **47,** 175 (1978).
53. G. Corongiu and E. Clementi, *Biopolymers,* **20,** 2427 (1981).
54. N. Metropolis, A.W. Rosenbluth, M.N. Rosenbluth, A.H. Teller and E. Teller, *J. Chem. Phys.,* **21,** 1087 (1953).
55. C. Pangali, M. Rao and B.J. Berne, *Chem. Phys. Lett.,* **55,** 413 (1978).
55. (b). M. Rao, C. Pangali and B.J. Berne, *Mol. Phys.,* **37,** 1773 (1979).
56. (a). J.C. Owicki and H.A. Scheraga, *Chem. Phys. Lett.,* **47,** 600 (1979).
56. (b). J.C. Owicki and H.A. Scheraga, *J. Am. Chem. Soc.,* **99,** 7413 (1977).
57. F.J. Millero, *J. Phys. Chem.,* **82,** 789 (1978).
58. F.J. Millero, in *Water and Aqueous Solutions,* R.A. Horne, Ed., Wiley Interscience, NY, 1972, p. 519.
59. J.E. Erpenbeck, W.W. Wood, in *Modern Theoretical Chemistry,* B.J. Berne, Ed., Plenum, New York, 1977, Vol. 6, Ch-2.
60. P.K. Mehrotra, M. Mezei and D.L. Beveridge, *J. Chem. Phys.,* **78,** 3156 (1983).
61. O. Matsuoka, E. Clementi and M. Yoshimine, *J. Chem. Phys.,* **72,** 3979 (1980).
62. D.L. Beveridge, M. Mezei, P.K. Mehrotra, F.T. Marchese, G. Ravishanker, T.R. Vasu and S. Swaminathan, in *Molecular Based study of Fluids,* J.M. Haile and G.A. Mansoori, Eds., American Chemical Society, 1983.
63. Gaussian-80, QCPE, adapted for IBM by S. Topiol and R. Osman.
64. O. Matsuoka, C. Tosi and E. Clementi, *Biopolymers,* **17,** 33 (1978).
65. H. Kistenmacher, H. Popkie and E. Clementi, *J. Chem. Phys,,* **59,** 5842 (1973).
66. M. Mezei and D.L. Beveridge, *J. Chem. Phys.,* **74,** 6902 (1981).
67. H. Kistenmacher, H. Popkie and E. Clementi, *J. Chem. Phys.,* **58,** 1689 (1973).
68. S. Swaminathan, S.W. Harrison and D.L. Beveridge, *J. Am. Chem. Soc.,* **100,** 5705 (1978).
69. P.K. Mehrotra and D.L. Beveridge, *J. Am. Chem. Soc.,* **102,** 4287 (1980).
70. M. Mezei and D.L. Beveridge, *Meth. in Enzymol.,* **27,** 21 (1986).
71. F.T. Marchese and D.L. Beveridge, *J. Am. Chem. Soc.,* **106,** 3713 (1984).
72. S.W. Harrison, M. Mezei and D.L. Beveridge, *Israel J. Chem.,* **27,** 163 (1986).
73. L.R. Pratt and D. Chandler, *J. Chem. Phys.,* **73,** 3430 (1980).
74. M. Mezei, P.K. Mehrotra and D.L. Beveridge, *J. Bio. Mol. Str. and Dynam.,* **2,** 1 (1984).
75. G.L. Seibel, U.C. Singh and P.A. Kollman, *Proc. Nat. Acad. Sci. USA,* **82,** 6537 (1985).
76. M. Mezei, P.K. Mehrotra and D.L. Beveridge, *J. Am. Chem. Soc.,* **107,** 2339 (1985).
77. G. Ravishanker, M. Mezei and D.L. Beveridge, *J. Comp. Chem.,* **7,** 345 (1986).
78. G.C. Piementel and A.C. McClellan, Hydrogen Bonding, W.H. Freeman, San Francisco, 1960.
79. H.G. Hertz and C. Raedle, *Ber. Bunsenges. Phys. Chem.,* **77,** 521 (1973).
80. R.G. Gordon, *Adv. Magn. Reson.,* **3,** 1 (1968).
81. H.G. Hertz, in *Water: A Comprehensive Treatise,* F. Franks, Ed., Plenum, New York, Vol. 3, Ch. 7.
82. H. Shindo, *Biopolymers,* **19,** 509 (1980).